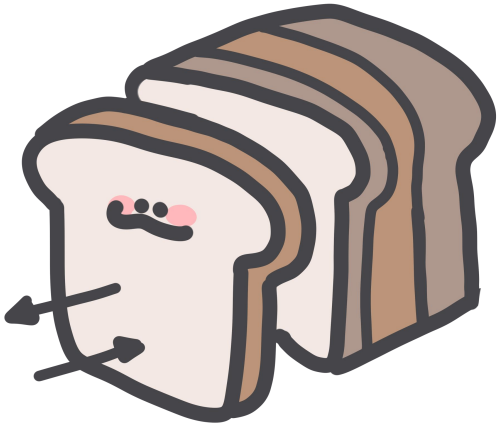

SlicedBREAD

Enhancing Axion Detection Efficiency in BREAD with Dielectric Stacks and Experimental Overview

I-see Jaidee , Grant McIntyre
Harvard University

Outline

- Dielectric Haloscope
  - Power Boost Factor Sensitivity Estimation
  - Stack Designs
- Experimental Overview
  - Optics Geometry Optimization
  - Wavefront simulation
- Result & Data Analysis
- Future Plans

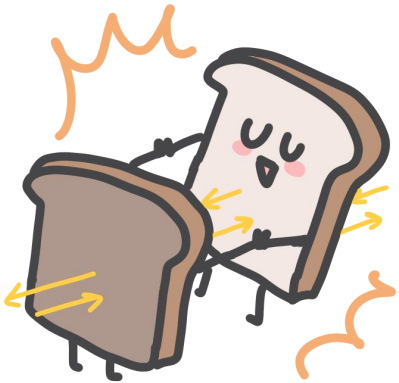

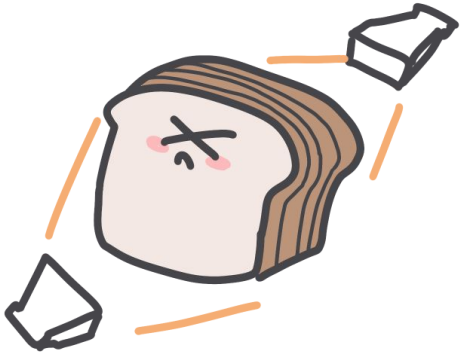

Dielectric Haloscope

https://arxiv.org/abs/1612.07057

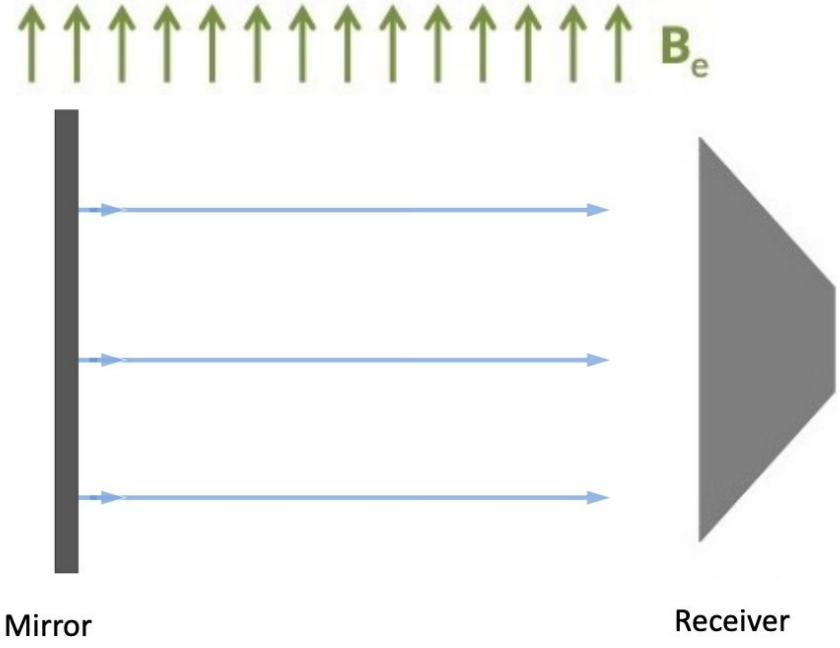

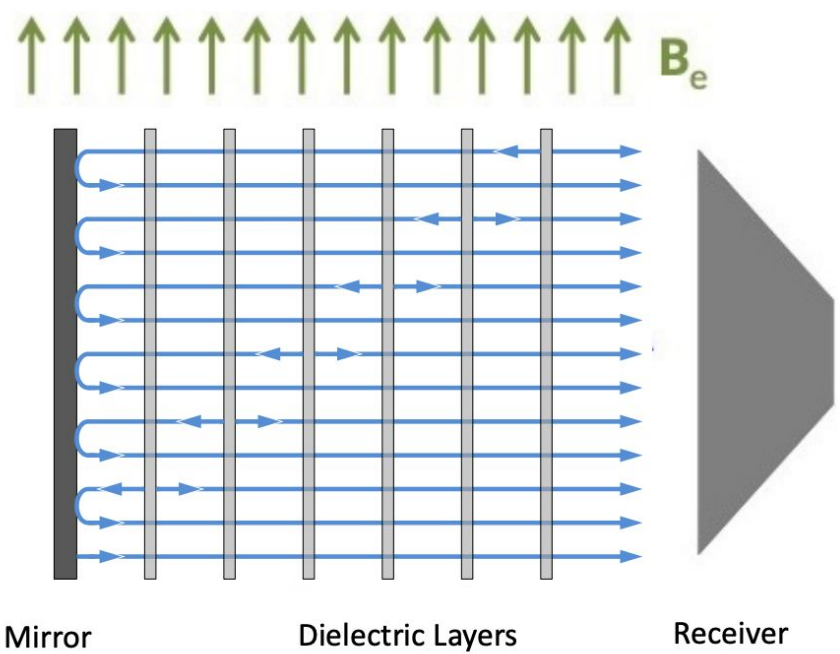

$$P_{\text{sig}} = \qquad P_{\text{dish}}$$

$$P_{\text{sig}} = \beta^2 \times P_{\text{dish}}$$

https://arxiv.org/abs/1611.05865

Axion-induced E field

Interaction term:

$$\mathcal{L}_{\text{int}} = g_{a\gamma}\, a\, \mathbf{E} \cdot \mathbf{B}$$

Ampere-Maxwell equation:

$$\nabla \times \mathbf{B} - \epsilon \frac{\partial \mathbf{E}}{\partial t} = g_{a\gamma} \left(\frac{\partial a}{\partial t} \mathbf{B} - \mathbf{E} \times \nabla a \right)$$

With B_e applied, the axion EM field sources a tiny electric field:

$$\mathbf{E}_a = -\frac{g_{a\gamma} \mathbf{B}_e}{\epsilon} a$$

Figure from Stefan

EM radiation at an interface

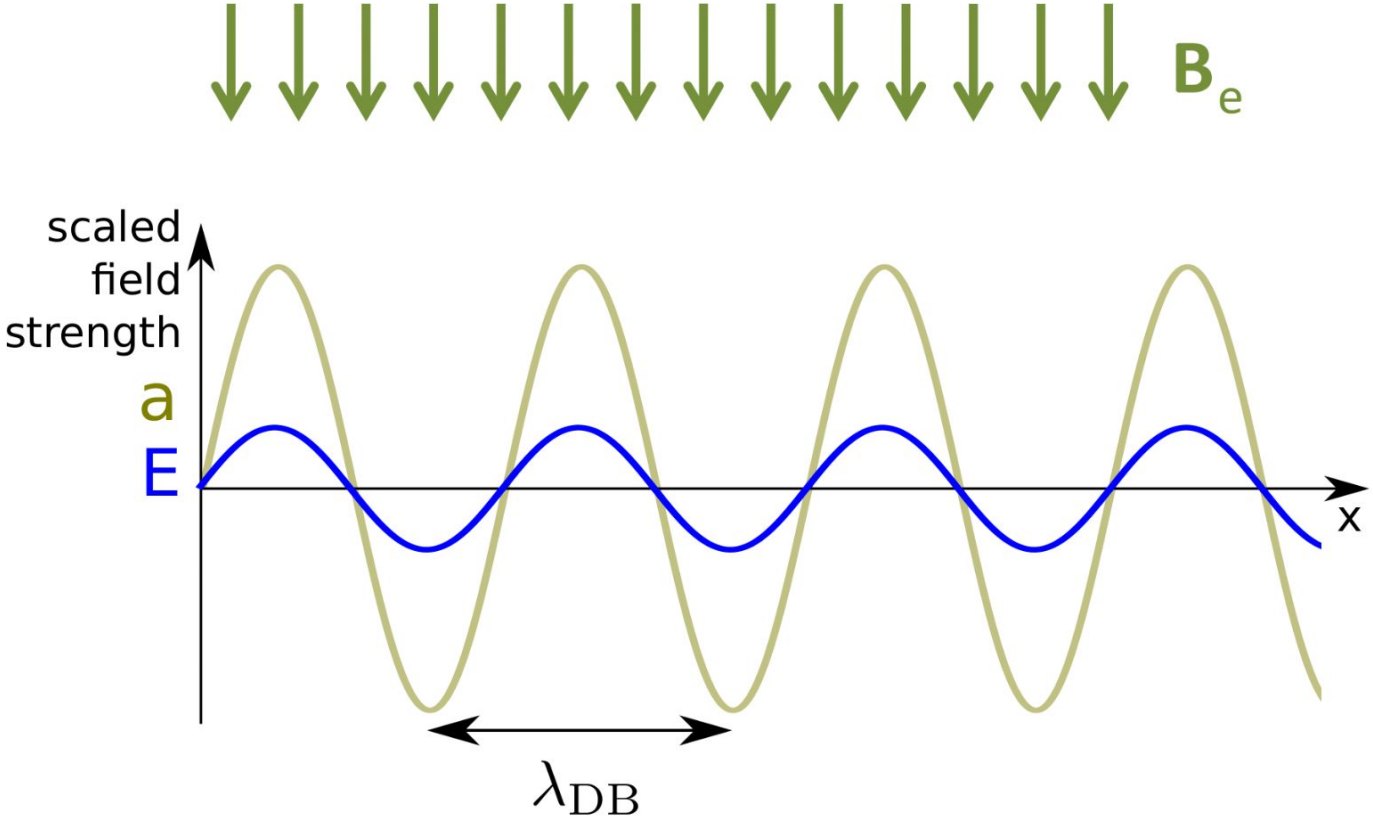

$$\mathbf{E}_a = -\frac{g_{a\gamma}\mathbf{B}_e}{\epsilon}a$$

$$a \propto \cos(m_a t)$$

Figure from Stefan

EM radiation at an interface

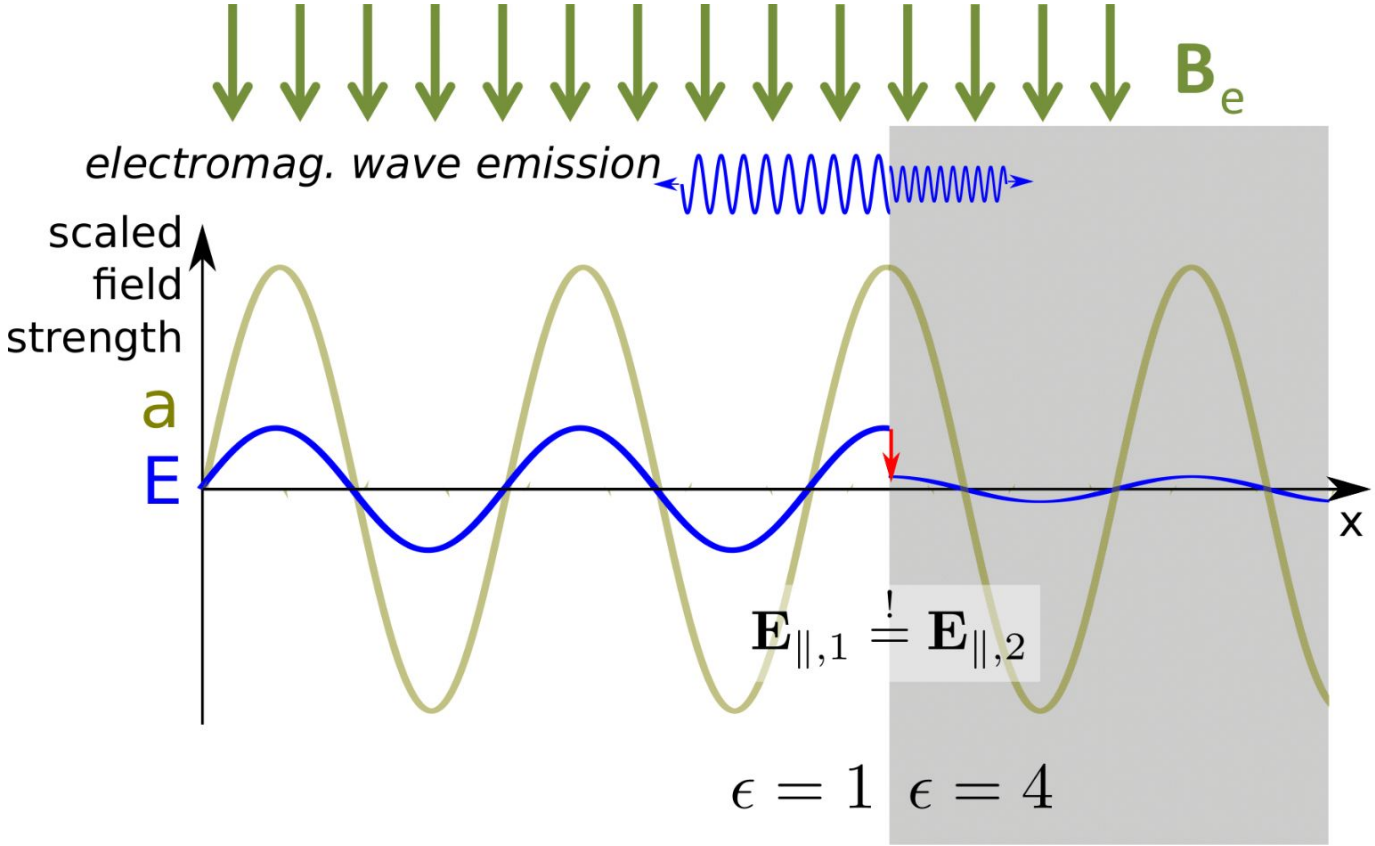

$$\mathbf{E}_a = -\frac{g_{a\gamma}\mathbf{B}_e}{\epsilon} a$$

Figure from Stefan

SlicedBREAD: Long-term prospect

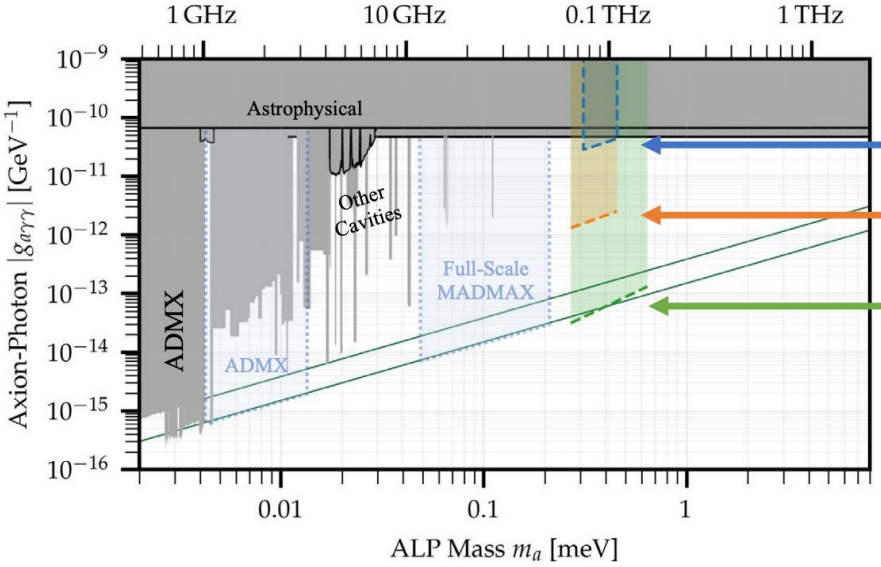

SlicedBREAD Phase I
at Harvard
A = 5e-3 m^2, B = 5T,
$\beta^2 \sim 30$ (5 disks)
HEMT amplifiers

SlicedBREAD Phase II
$A = 2\mathrm{m}^2, B = 9.4\mathrm{T},$
$\beta^2 \sim 100$
off-the-shelf amplifiers

SlicedBREAD Phase III
$A = 7\mathrm{m}^2, B = 20\mathrm{T},$
$\beta^2 \sim 1{,}000$
quantum limited amplifier

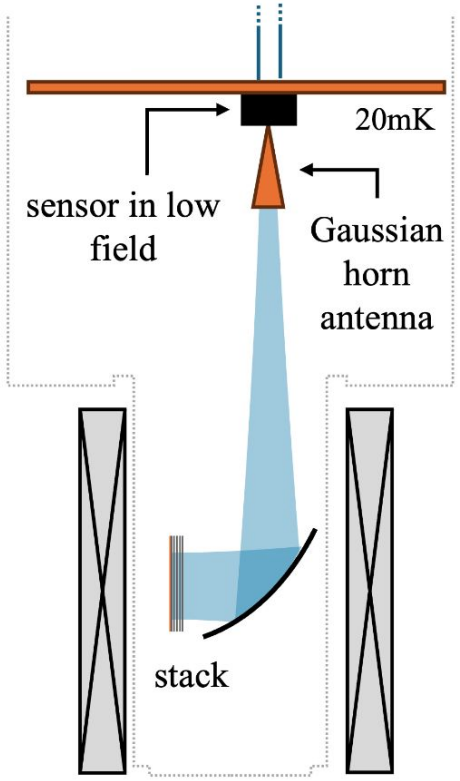

Stack Design for Testing

- Number of disk
- Dielectric constant
- Disk thickness
- **Disk spacing**

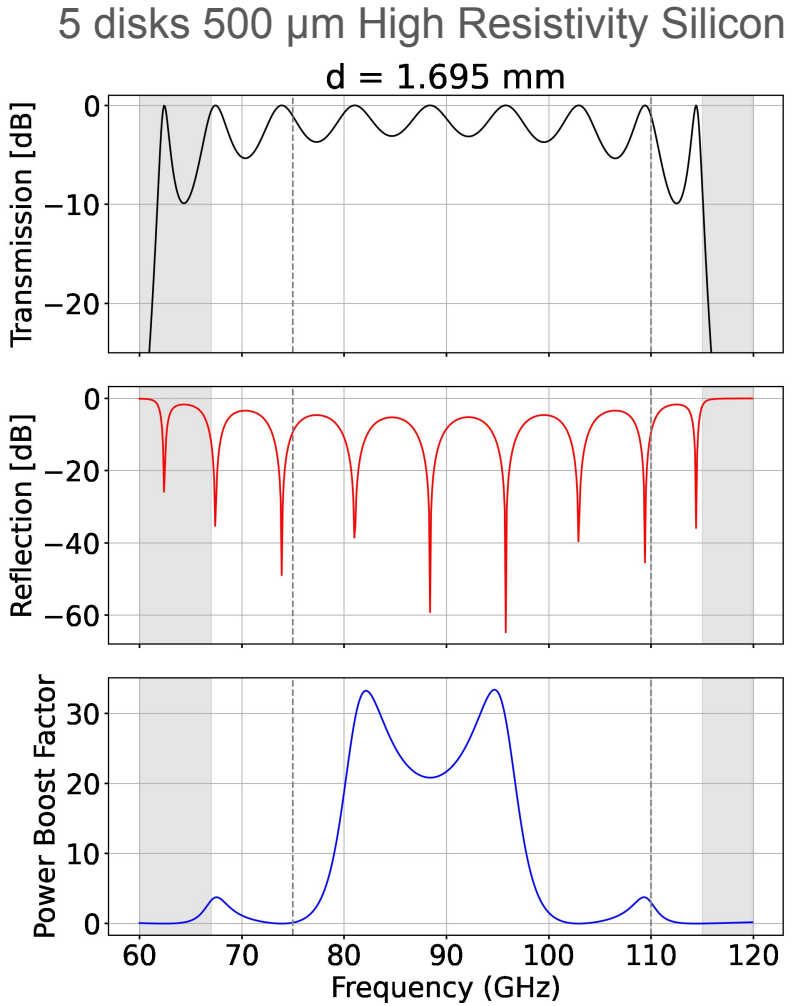

1 disk 500 um HR Si

ε = 11.5
Thickness = 500 μm

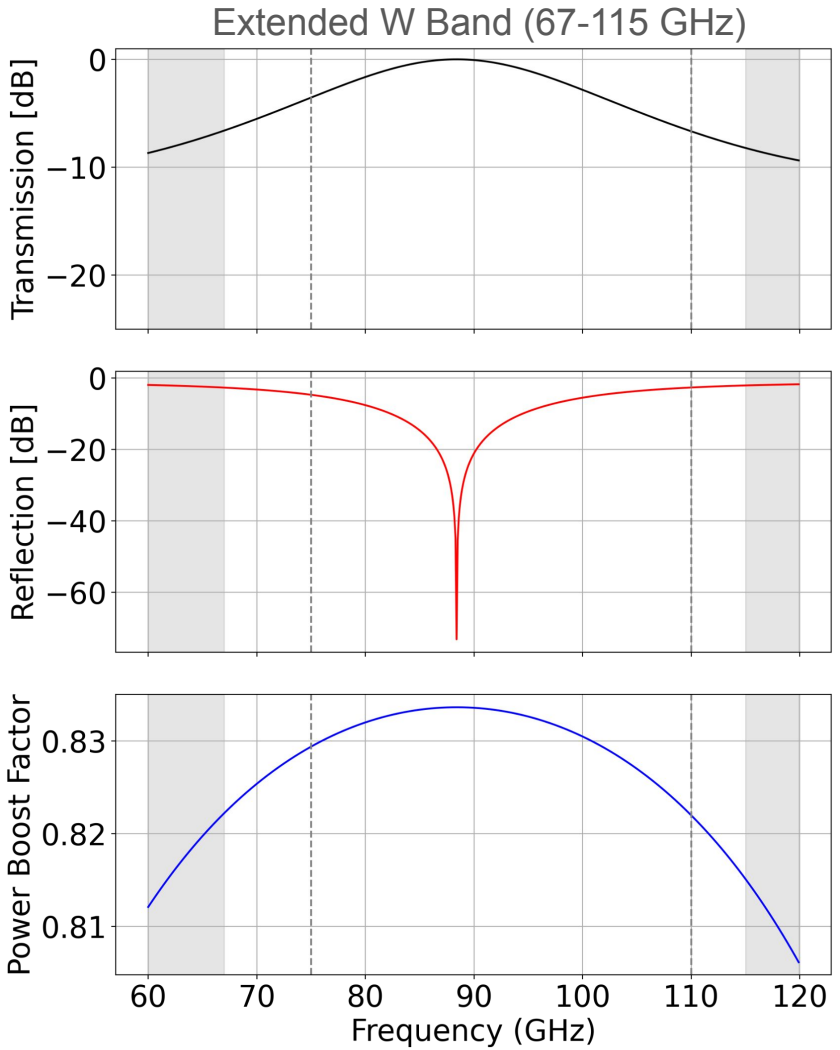

2 disks 500 um HR Si, d = 1.695 mm

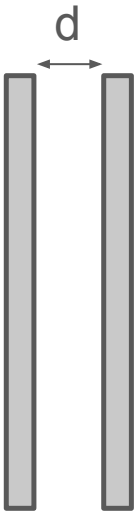

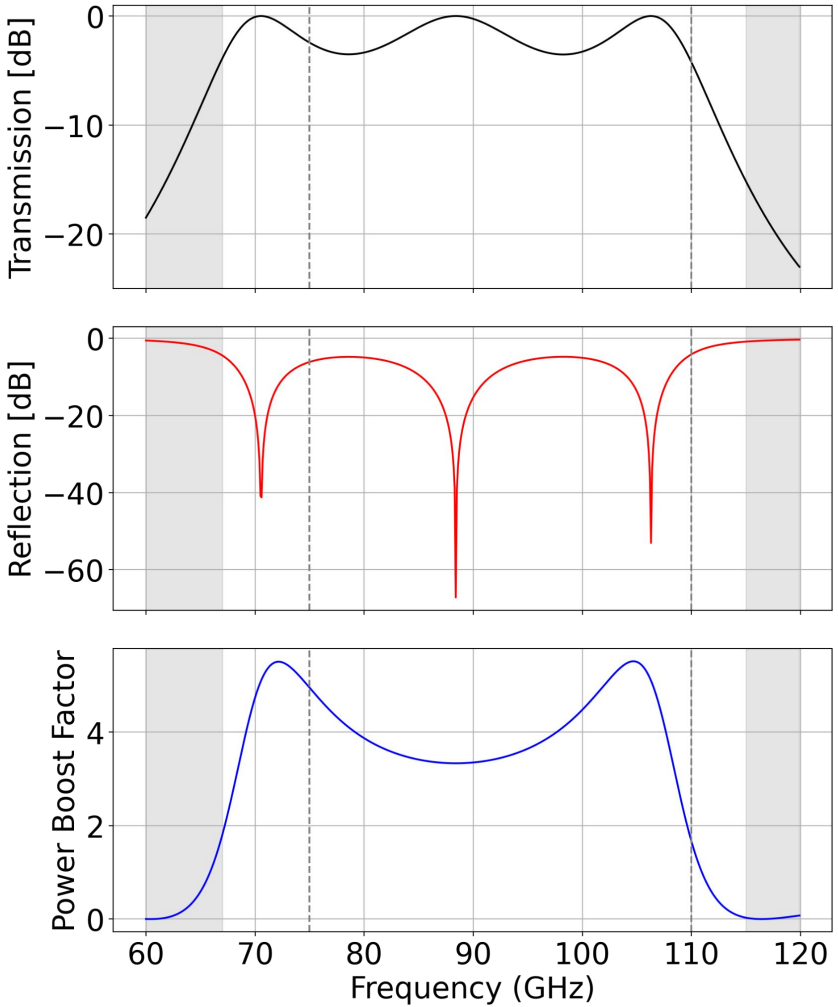

3 disks 500 um HR Si, d = 1.695 mm

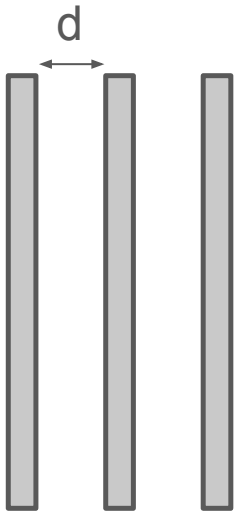

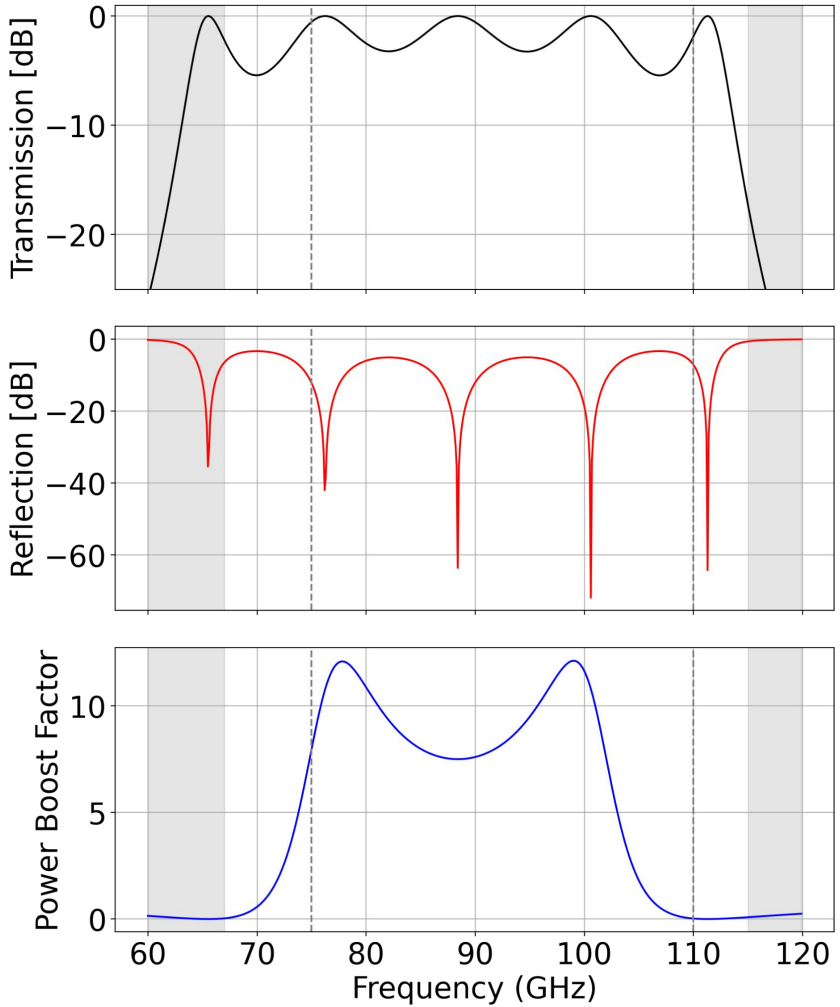

4 disks 500 um HR Si, d = 1.695 mm

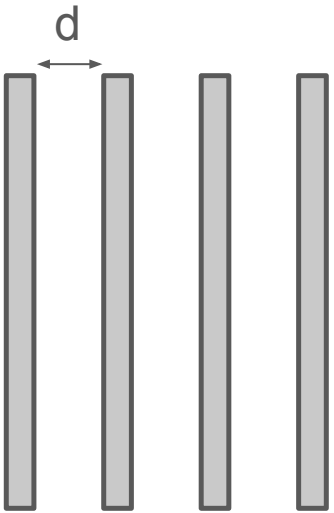

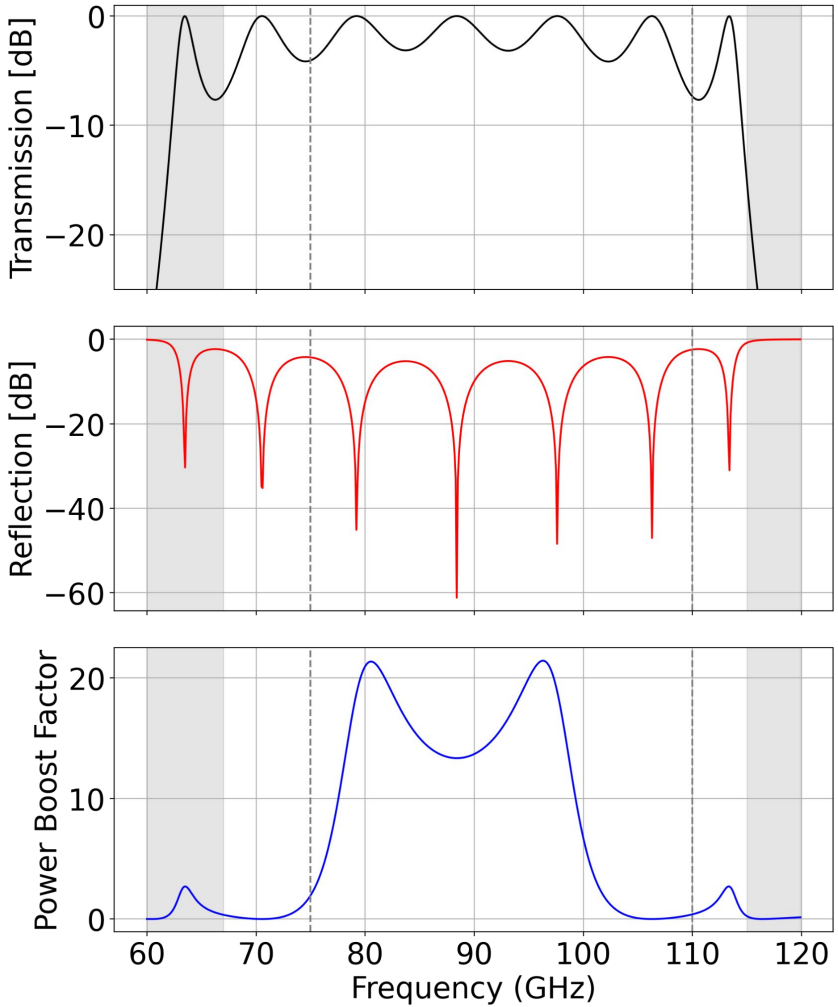

5 disks 500 um HR Si, d = 1.695 mm

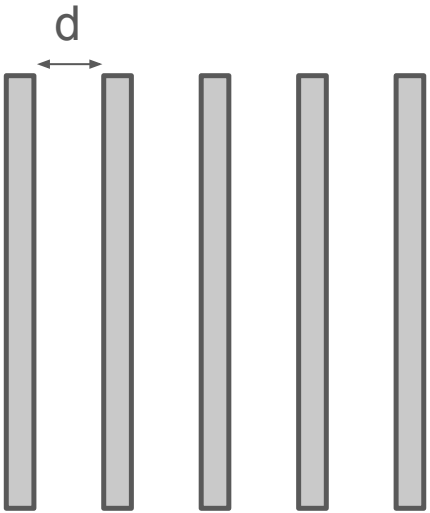

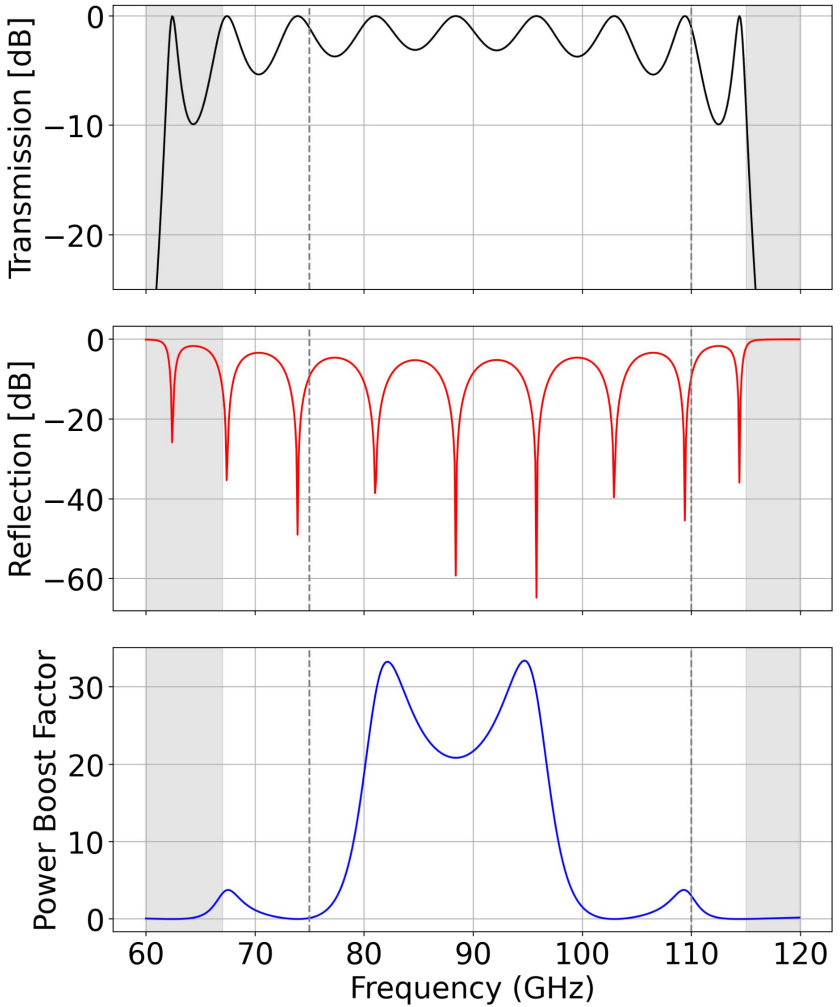

Sensitivity Estimation

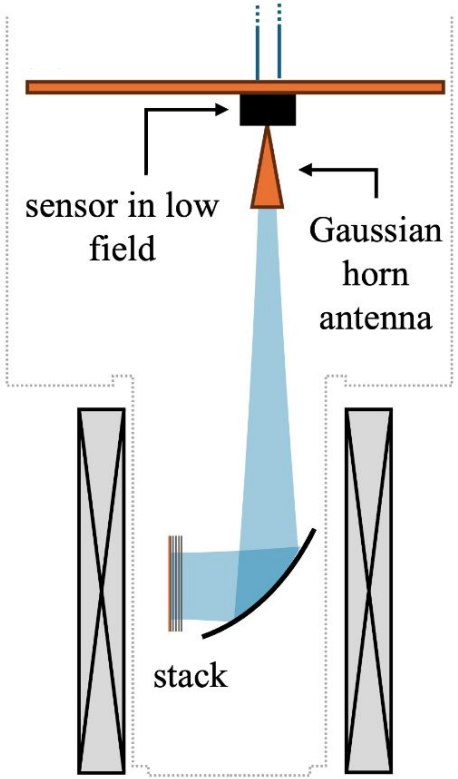

Disk Diameter = 3 inches
Magnetic field = 8T
Duration = 2 months
Signal-to-noise ratio = 5

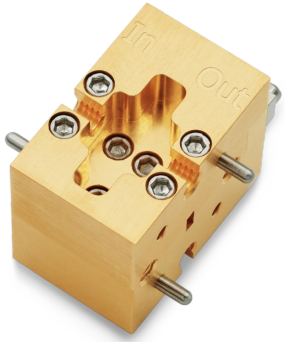

LNF-LNC65_115WB

Sensitivity Estimate for 5 disks 500 μm HR Si, 1.695 mm vacuum gap

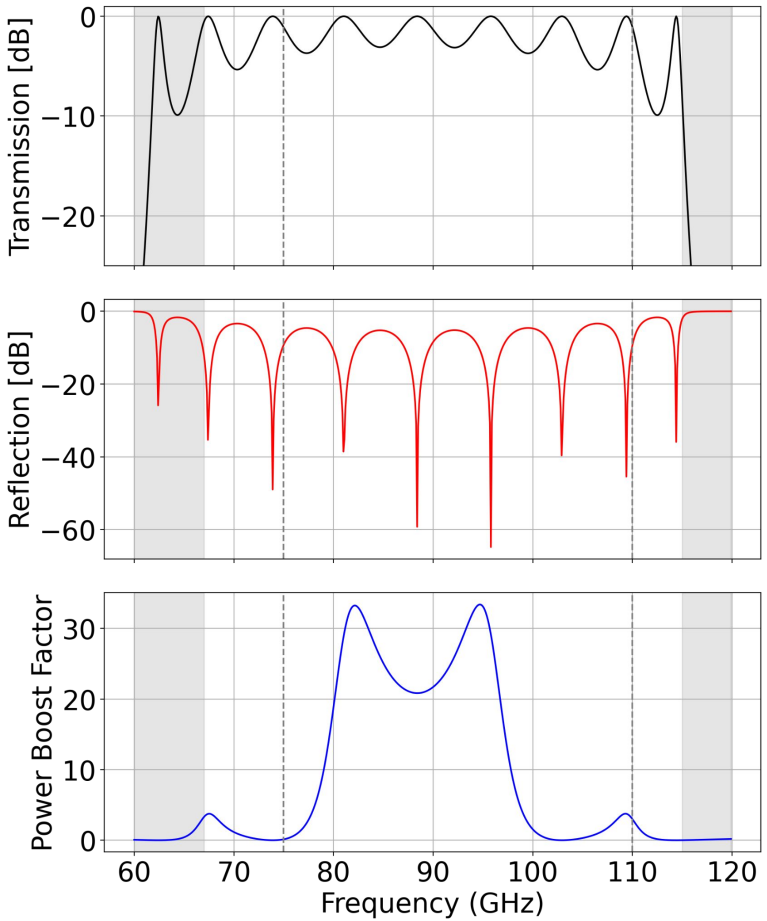

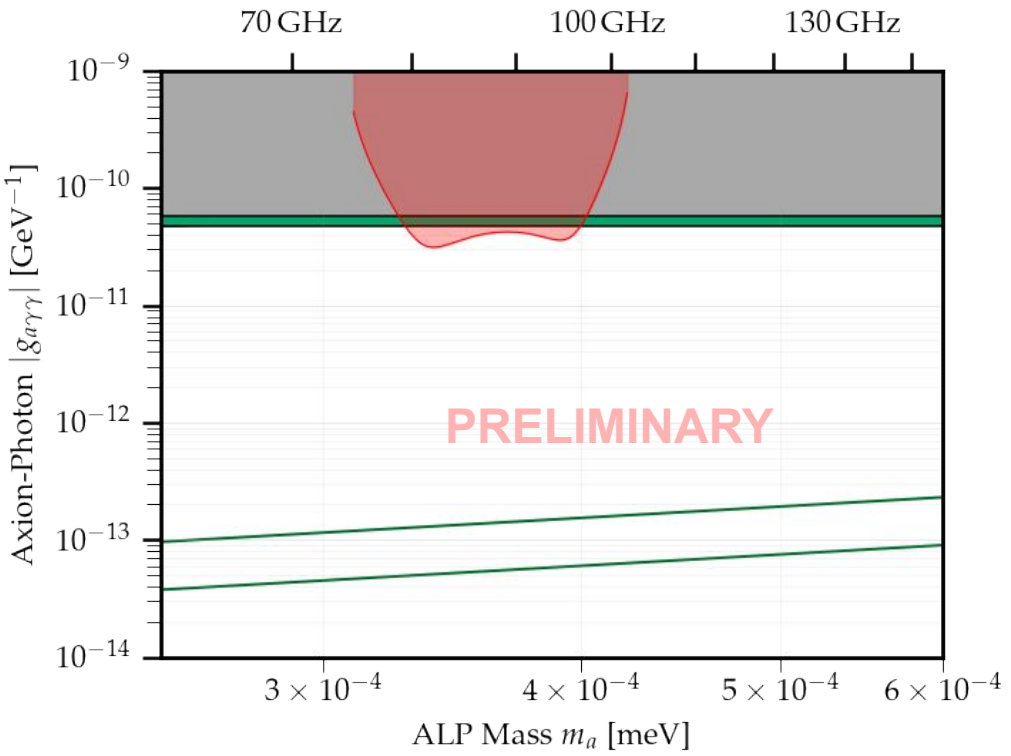

Sensitivity Estimate for 10 disks 500 μm HR Si, 1.695 mm vacuum gap

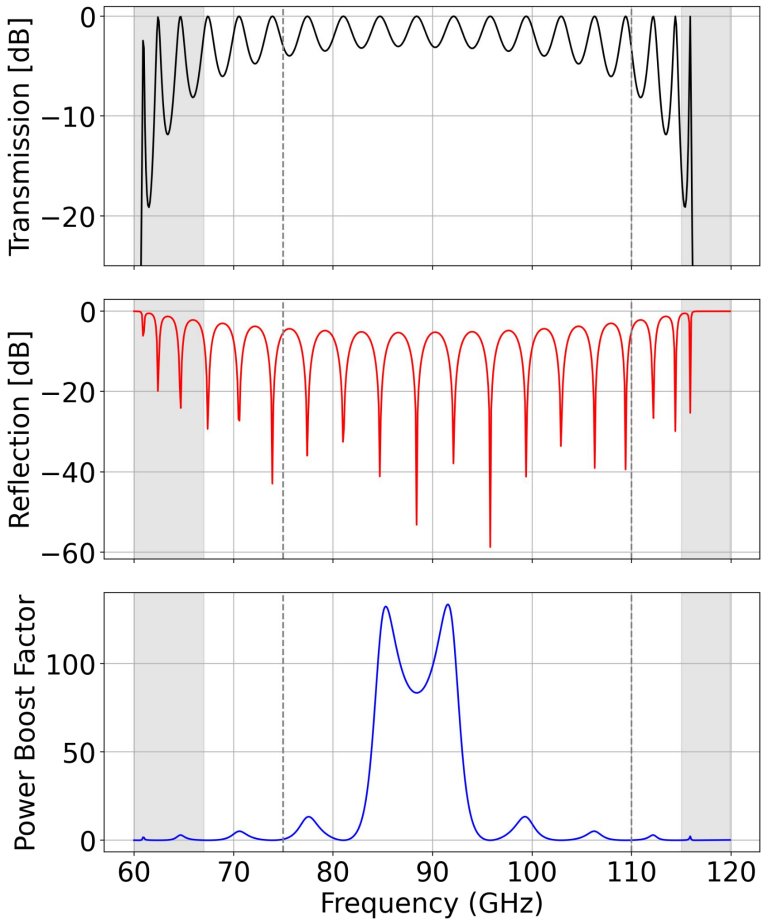

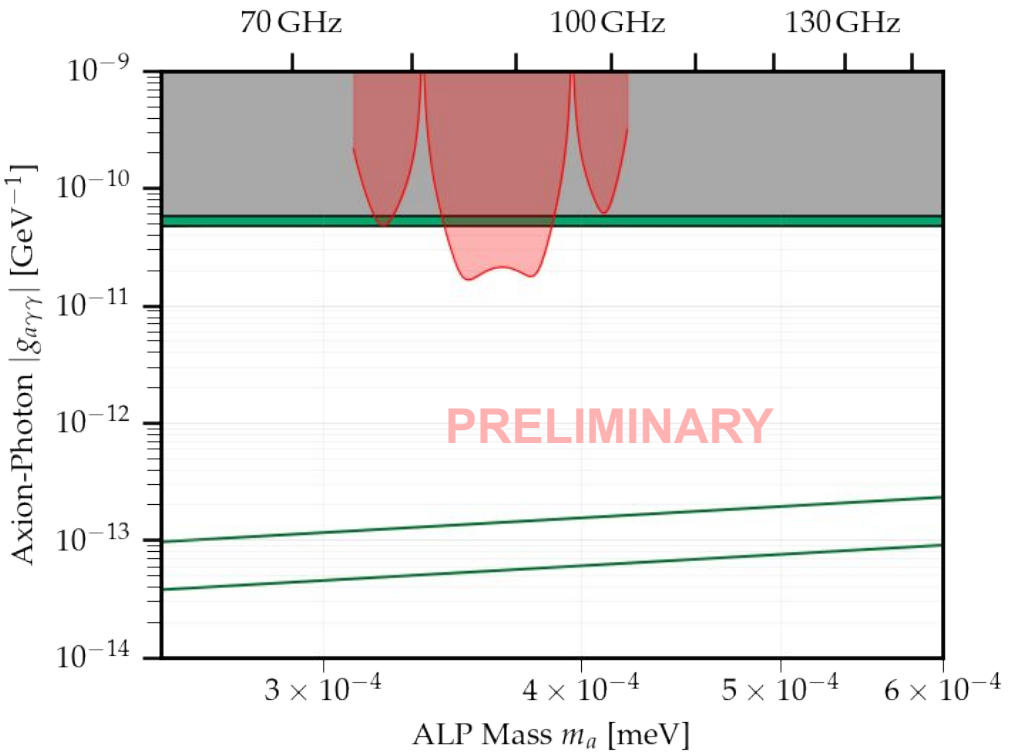

Sensitivity Estimate for 10 disks 500 μm HR Si, 2 mm vacuum gap

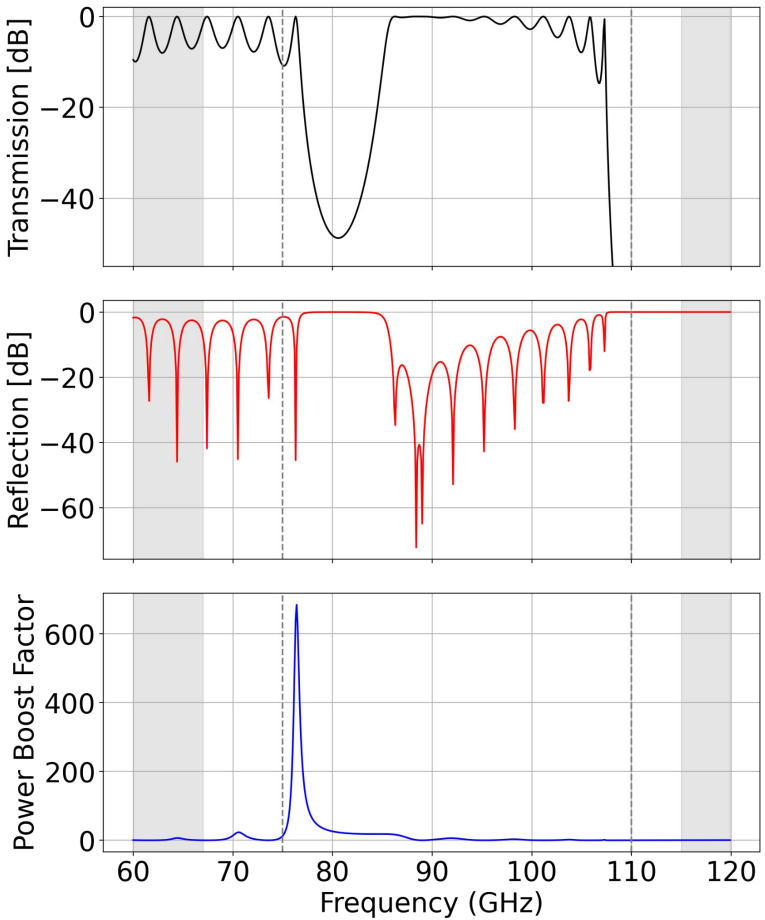

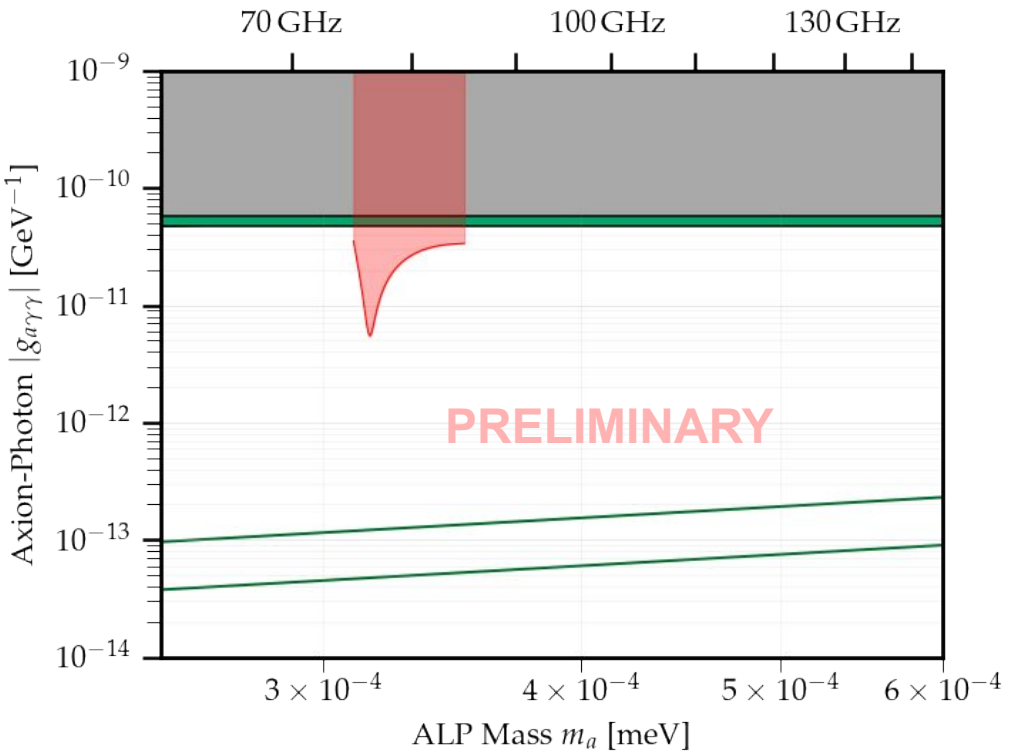

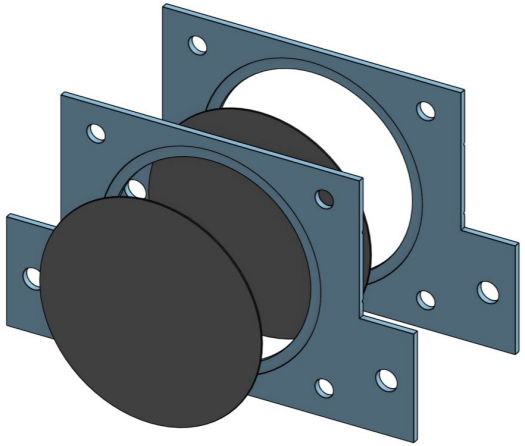

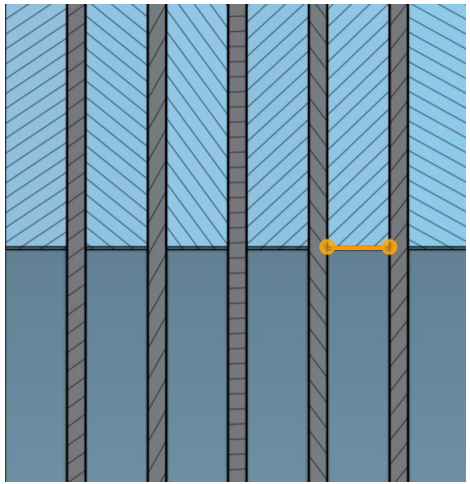

500 um disk thickness
1.695mm vacuum gap

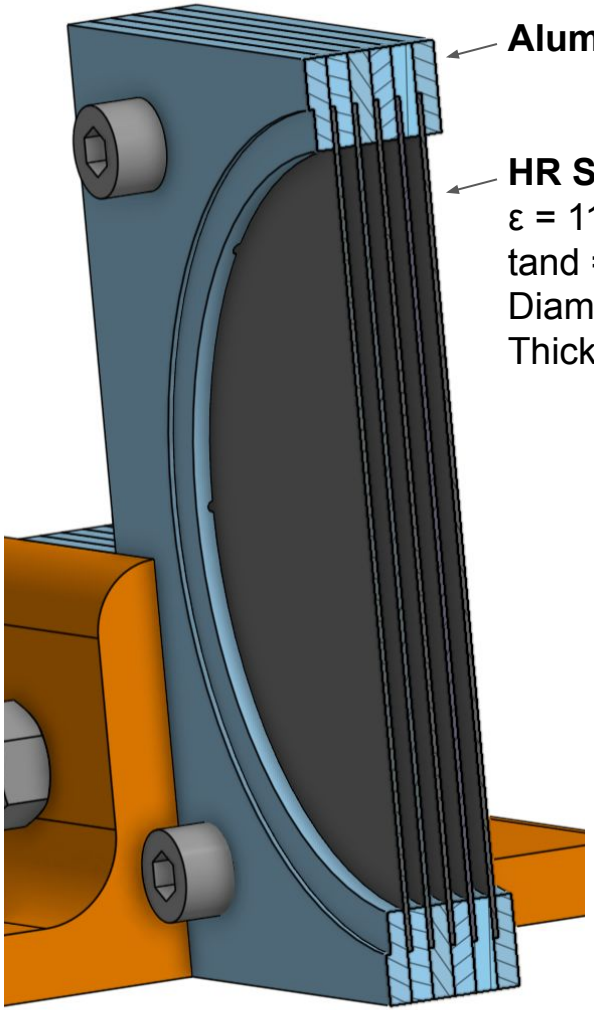

Aluminum 6061-T6x

HR Silicon (>10000 ohm-cm)
ε = 11.5
tand = 1.00E-06
Diameter = 76.2mm (3 in)
Thickness = 500 μm

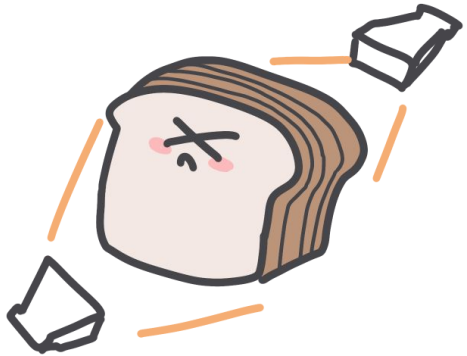

Sensitivity to uncertainty in spacers' thicknesses

For 0.13 mm mechanical tolerance

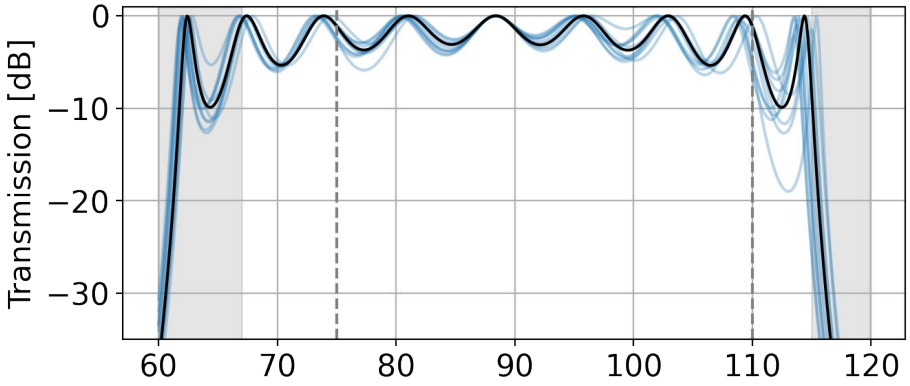

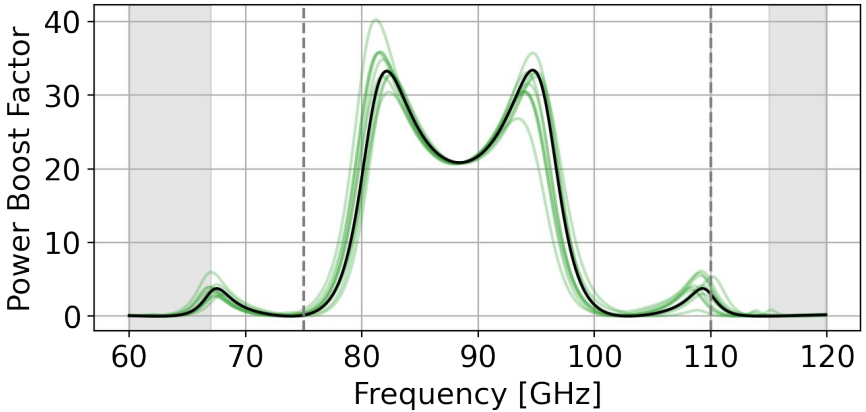

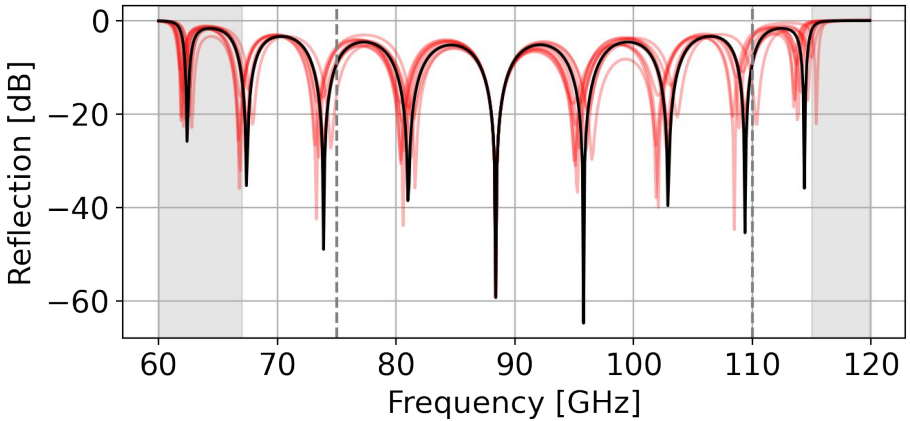

Sensitivity to angle misalignment

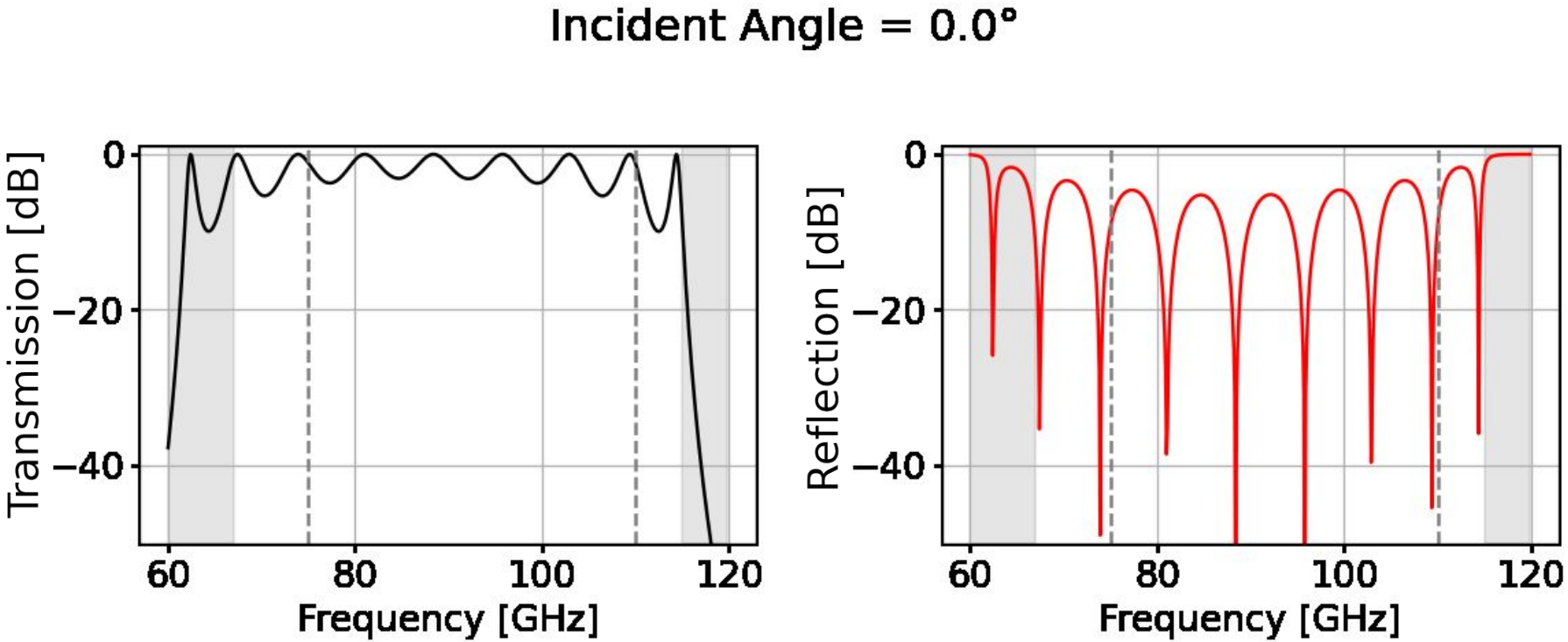

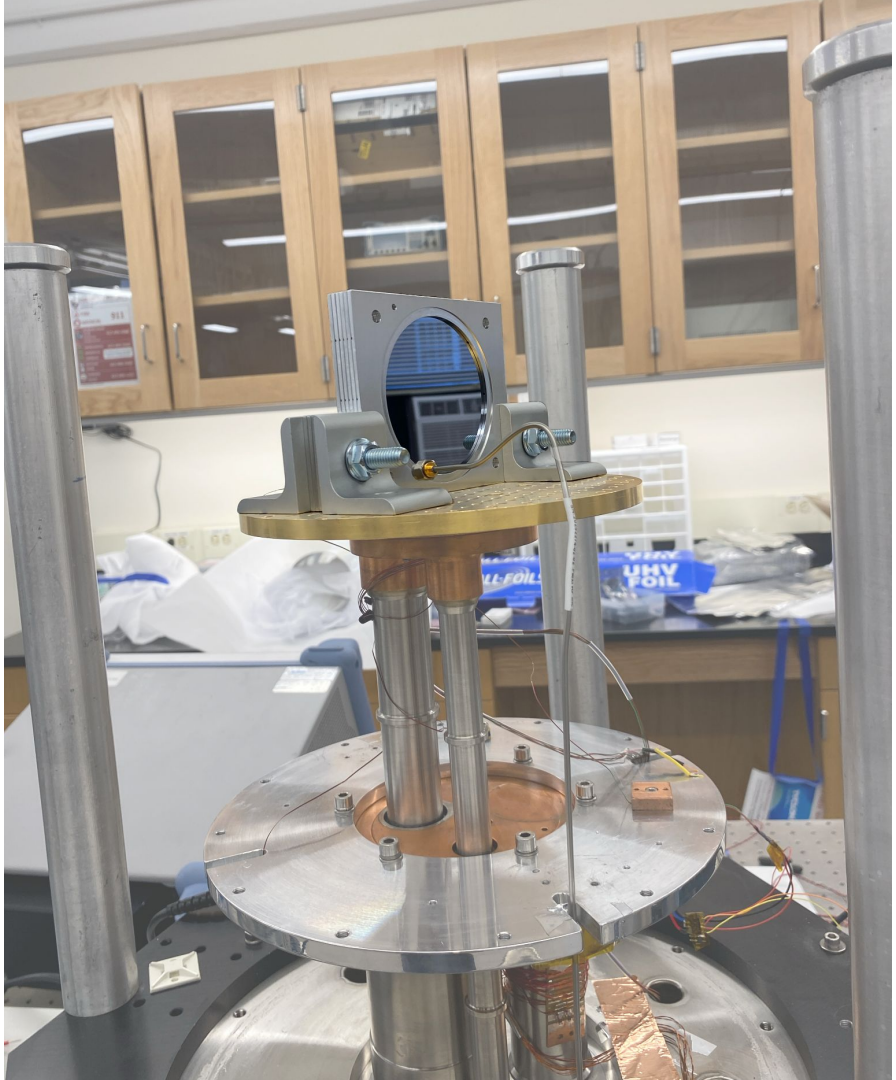

An air vent for outgassing

Hole for temperature sensor

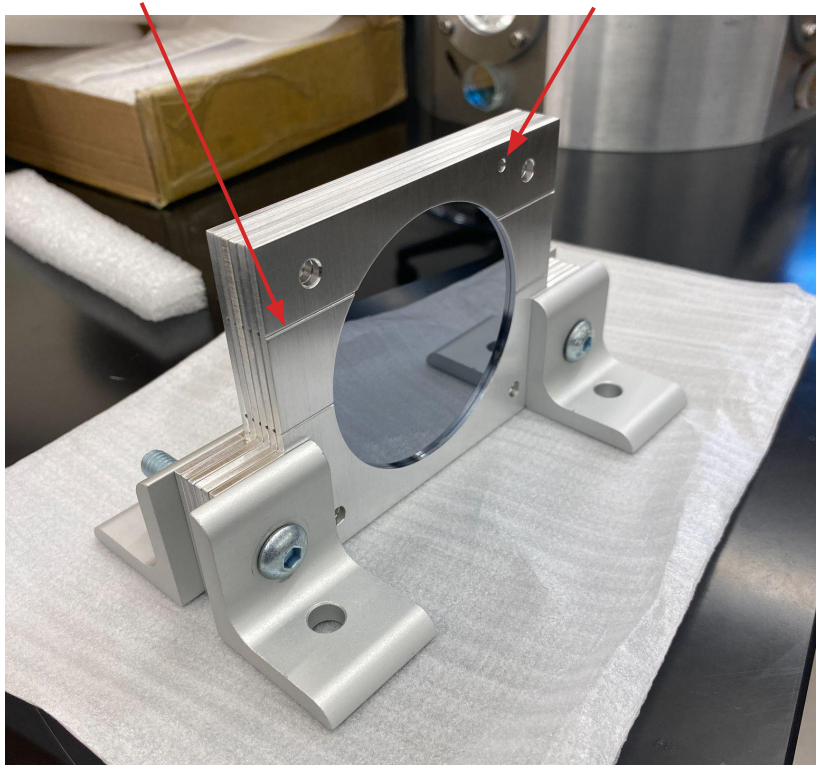

SlicedBREAD: Experimental Overview

Grant McIntyre
Harvard University

BREAD Collaboration Meeting
1/14/26

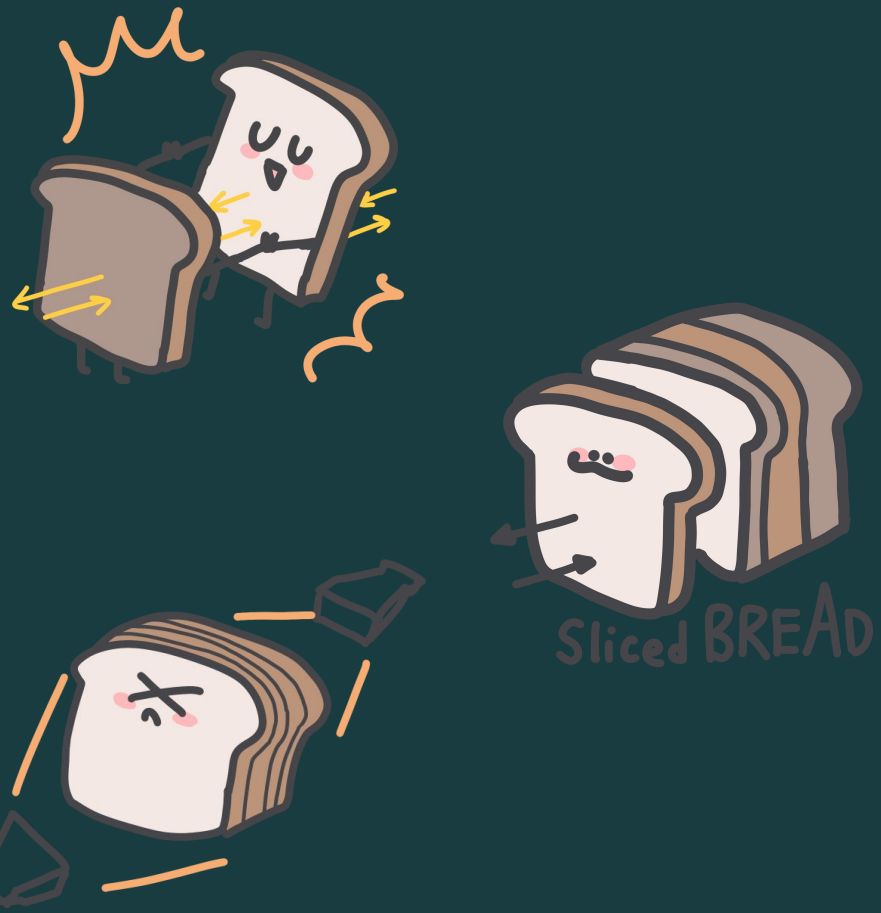

Content Overview

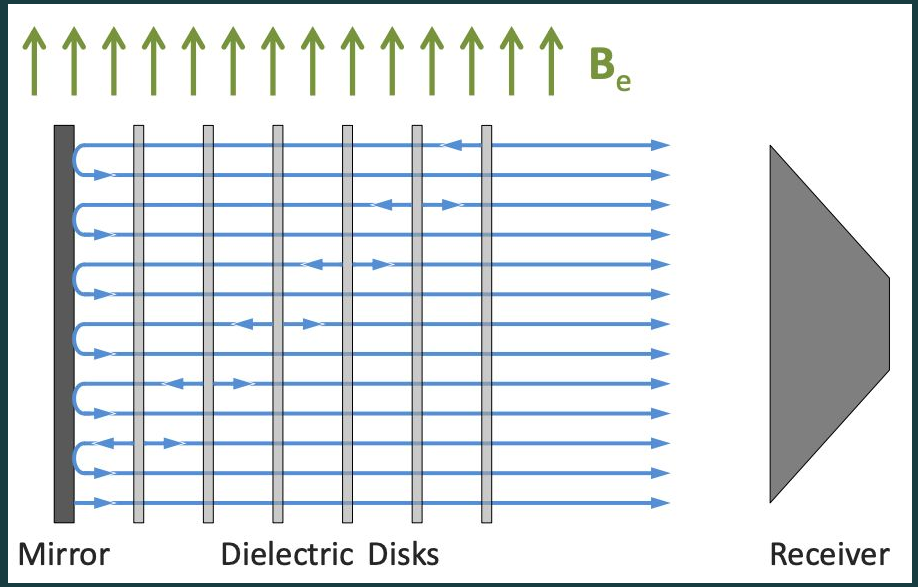

Fig. 1. A dielectric haloscope consisting of a mirror and several dielectric disks placed in an external magnetic field. Credit to the MADMAX Collaboration [1].

SlicedBREAD: Next Generation Dielectric Haloscope

- Axion DM converts into photons in the presence of B, producing tiny oscillating E
- Axion dark matter converts into photons in the presence of B, producing tiny oscillating E
- Tuning the disk geometry lets us scan over axion masses

End Goal: Combine with reflector to increase sensitivity

Initial Testing Goals:

1. Develop 75–110 GHz (W Band) cryogenic testbed for stack designs
2. Track S parameters and isolate stack effects on data
3. Compare to simulations to determine axion signal power boost

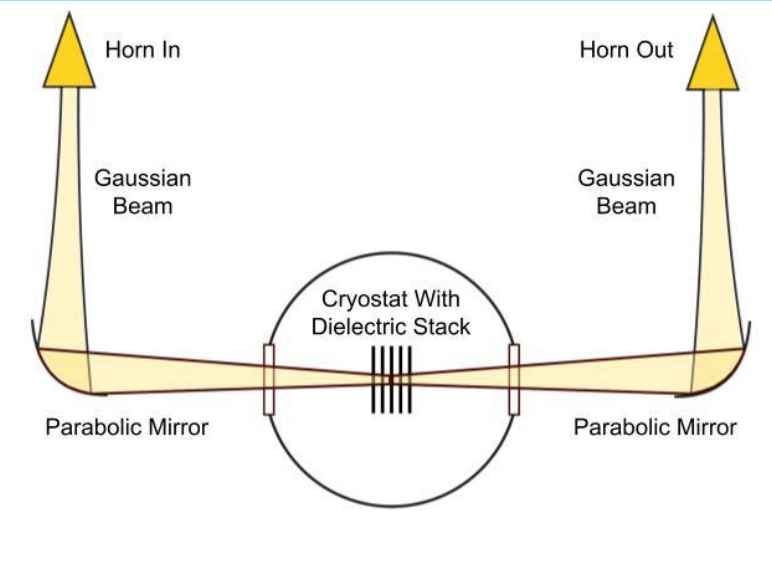

Fig. 2. A testbed to measure transmission and reflection of a mm-wave beam through a stack of dielectrics within a 4 K cryostat.

Experimental Setup

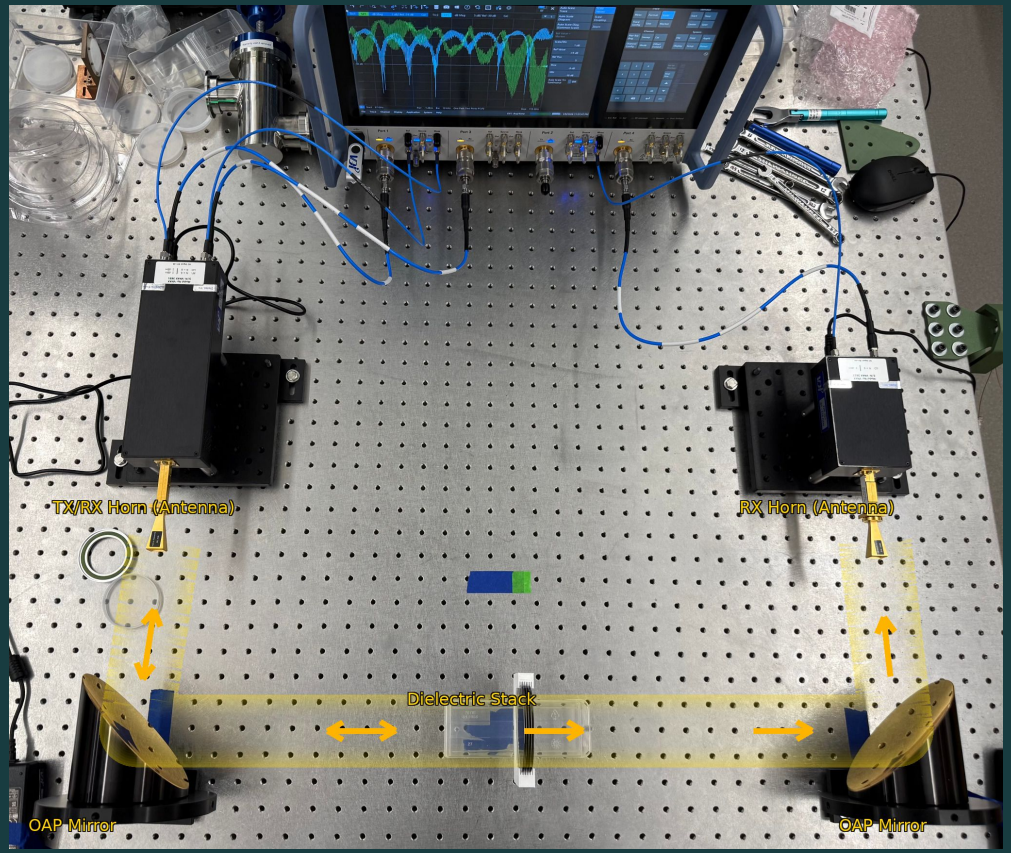

Materials:

R&S ZNA43

VDI W-Band Frequency Extenders

20 dBi Horn Waveguide Antenna

90° Off-axis Parabolic Mirrors

.5 mm thick High Resistivity Silicon

Optics Geometry Optimization

- Primary Concern: Truncation at cryostat window (r = 25 mm)
- Expect substantial diffraction effects when $r/\omega \leq 2$
- Stack to window distance (140 mm) $\rightarrow \omega_{window} \leq 18.85$ mm (75 GHz)

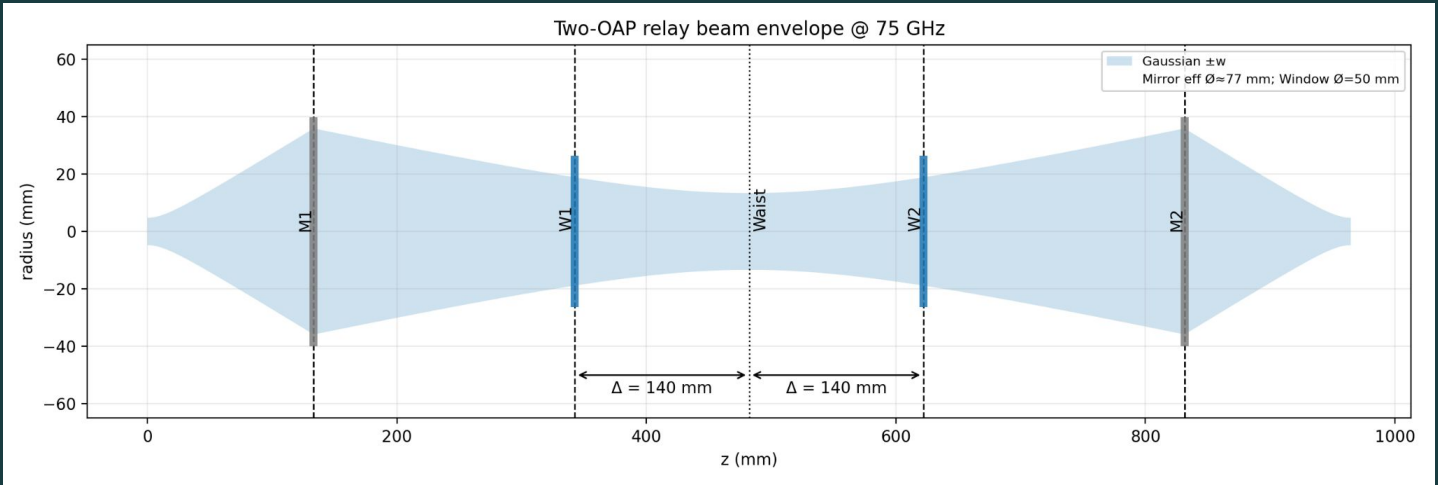

Fig. 3. Optimal 75 GHz optics geometry to obtain minimum beam radius at cryostat windows. Beam radii calculated assuming symmetric gaussian distribution with cut off at $1/e^2$ radius.

Optics Geometry Optimization

- Primary Concern: Truncation at cryostat window (r = 25 mm)
- Expect substantial diffraction effects when $r/\omega \leq 2$
- Stack to window distance (140 mm) $\rightarrow \omega_{window} \leq 18.85$ mm (75 GHz)

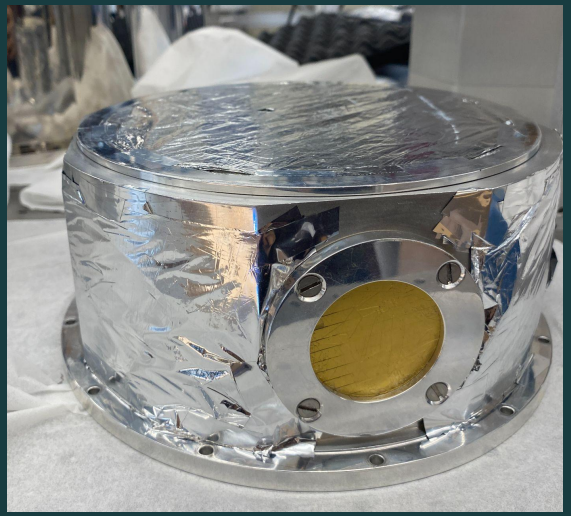

Diffraction Effects:

Simulated effects of diffraction on wavefront shape

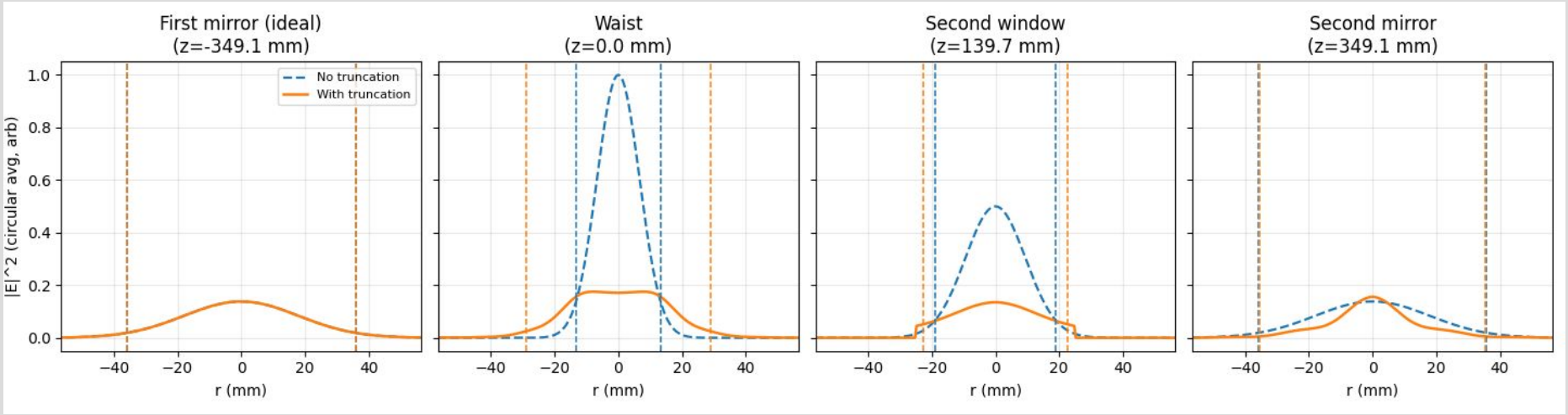

Fig. 4. Circularly averaged power distribution of gaussian beam at different points along the optical axis. Orange indicates distributions with diffraction effects, and blue is the beam without truncation. Vertical lines indicate 1/e^2 power boundary.

Diffraction Effects:

Simulated effects of diffraction on wavefront shape

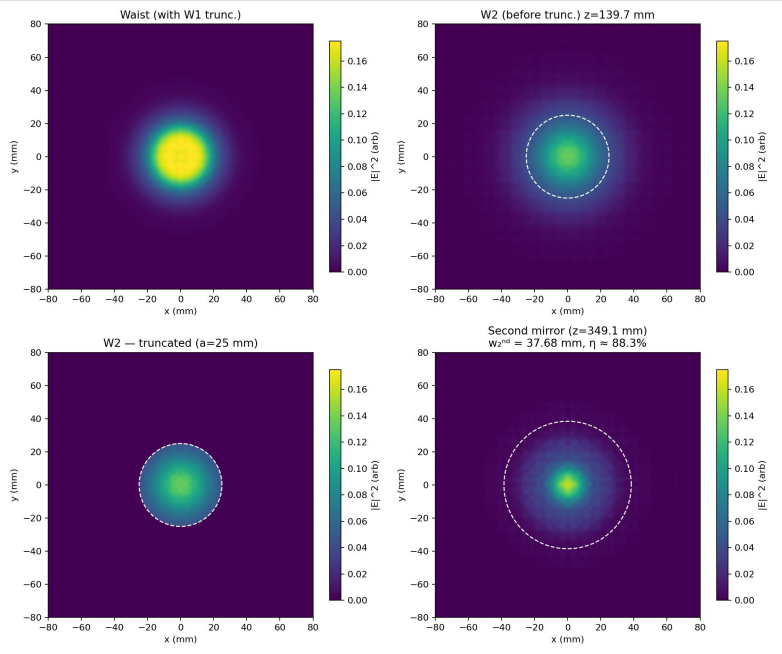

Fig. 5. Transverse intensity |E|^2 at key planes along the optical axis. The top-left panel shows the waist plane.

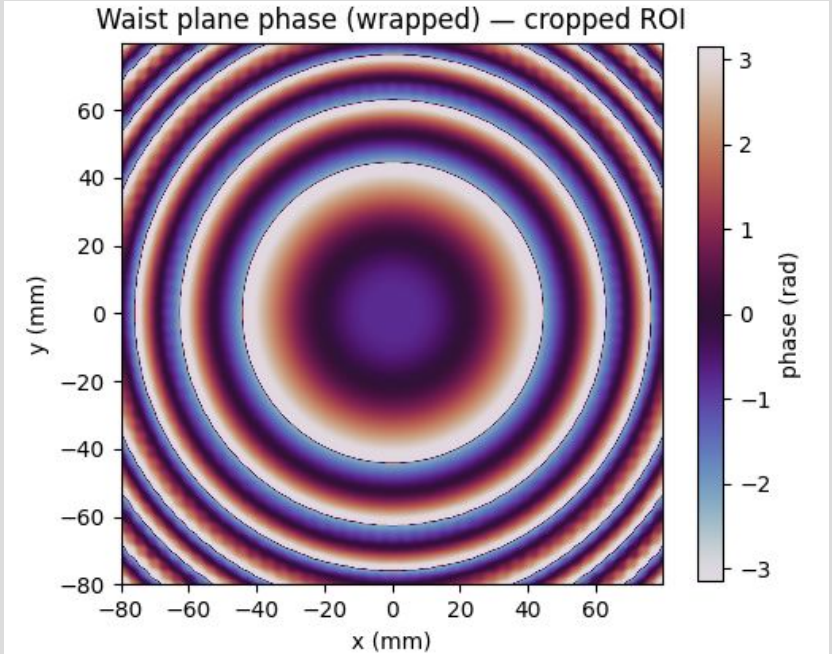

Fig. 6. Wrapped phase of the field at the waist plane after truncation. Ideally flat at center.

Experimental Results

All results from tests done with a 3D printed holder for 0.5 mm dielectric plates. Plates spaced with 1.695 mm ±0.25 mm between interfaces

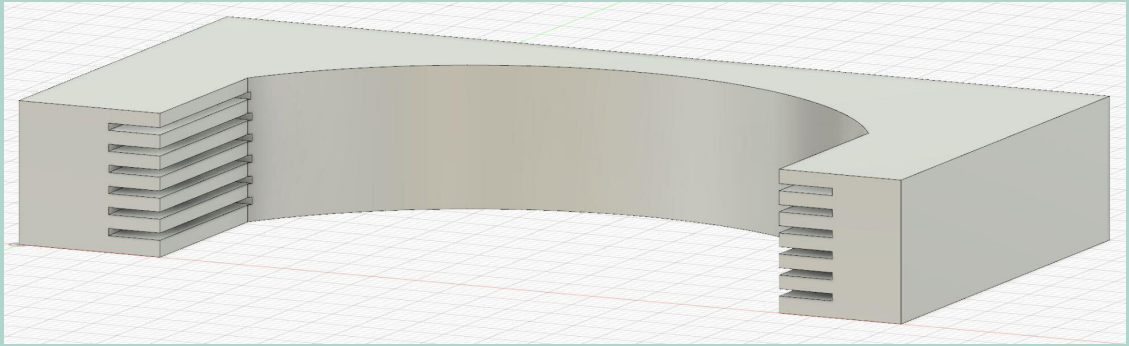

Raw Results (High Resistivity Si)

2 Plates

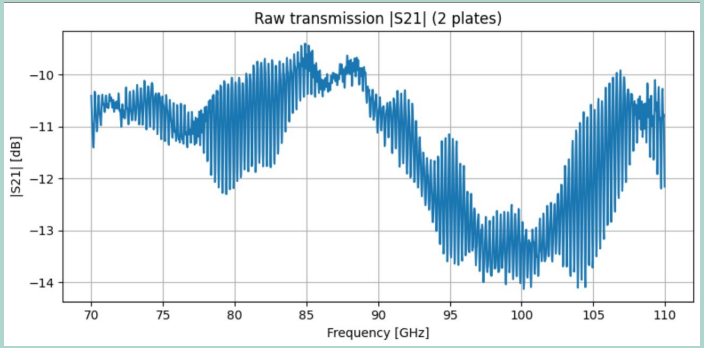

Fig. 7. Raw transmission data with 2 plates of high resistivity Si.

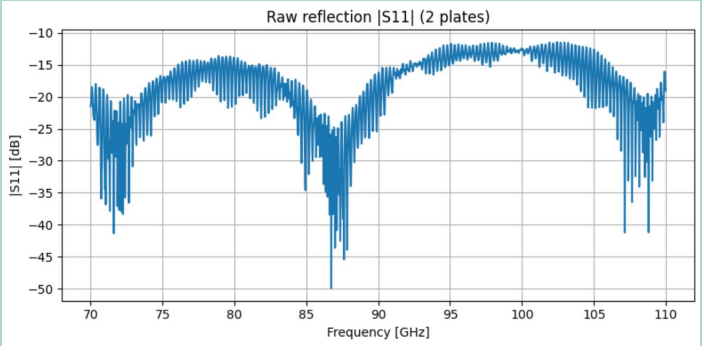

Fig. 8. Raw reflection data with 2 plates of high resistivity Si.

5 Plates

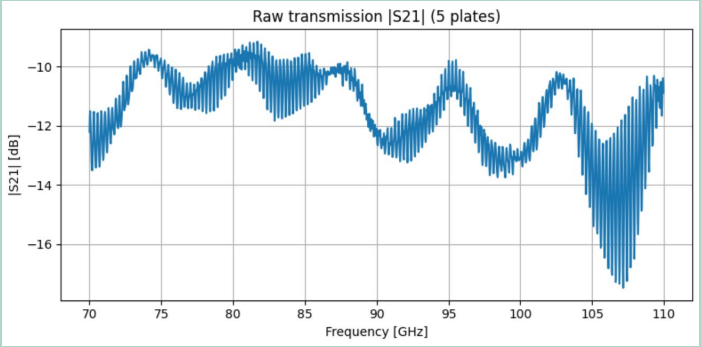

Fig. 9. Raw transmission data with 5 plates of high resistivity Si

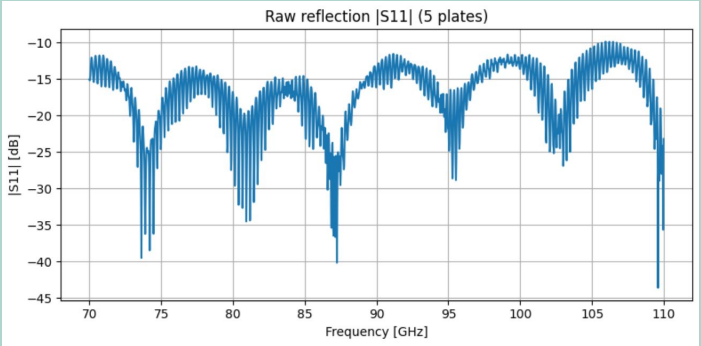

Fig. 10. Raw reflection data with 5 plates of high resistivity Si

Analysis Techniques

- Primary analysis conducted with time gating and normalization
- Allows systematic removal of unwanted reflection effects
- Primarily effective for reflection data

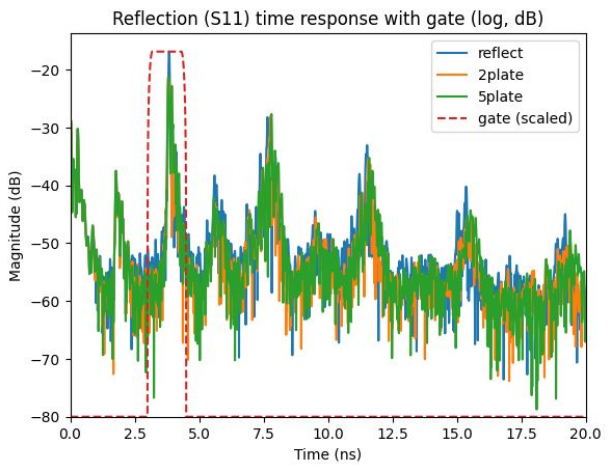

Fig. 11. Fourier transformed reflection data for reflector, 2 plates, and 5 plates of high resistivity Si. A time gate (red) is placed around the strongest peak. Gate applied to all S11 data.

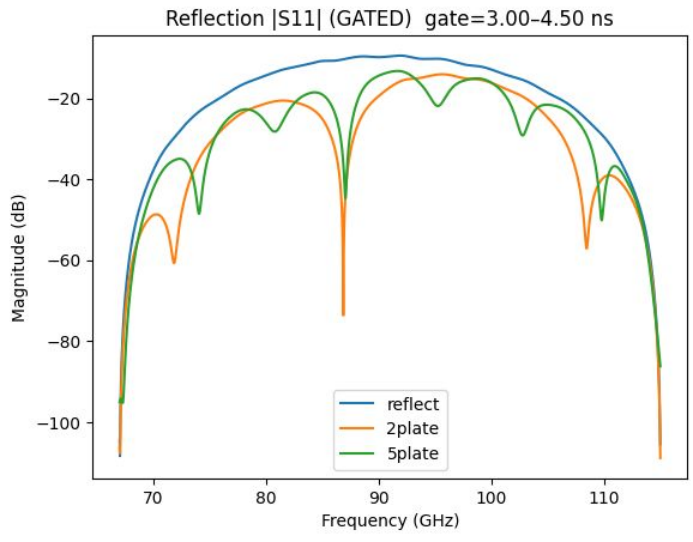

Fig. 12. Gated reflection data for reflector, 2 plates, and 5 plates. Tapers at edges due to applied Hann window to limit edge discontinuity effects on FFT.

Analysis Results

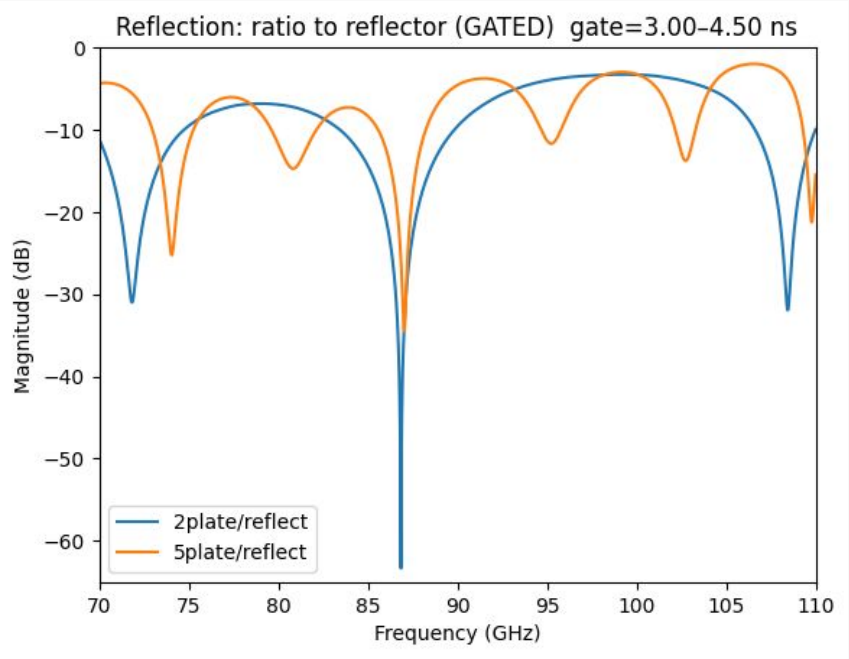

Fig. 13. Reflection data time gated and normalized. 2 plate data in blue, and 5 plate data in orange.

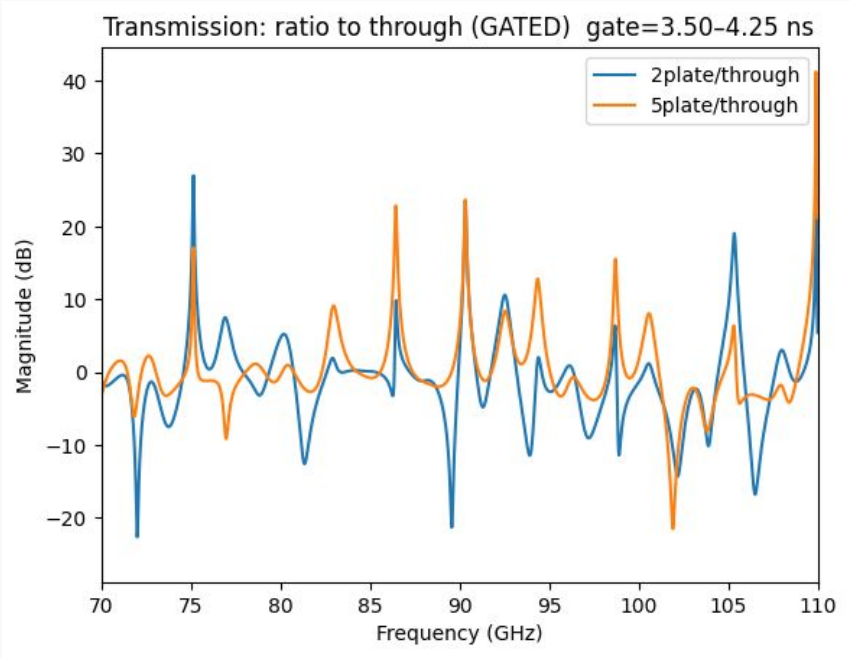

Fig. 14. Transmission data time gated and normalized. 2 plates data in blue, and 5 plate data in orange.

Comparison to Simulations (2 plates)

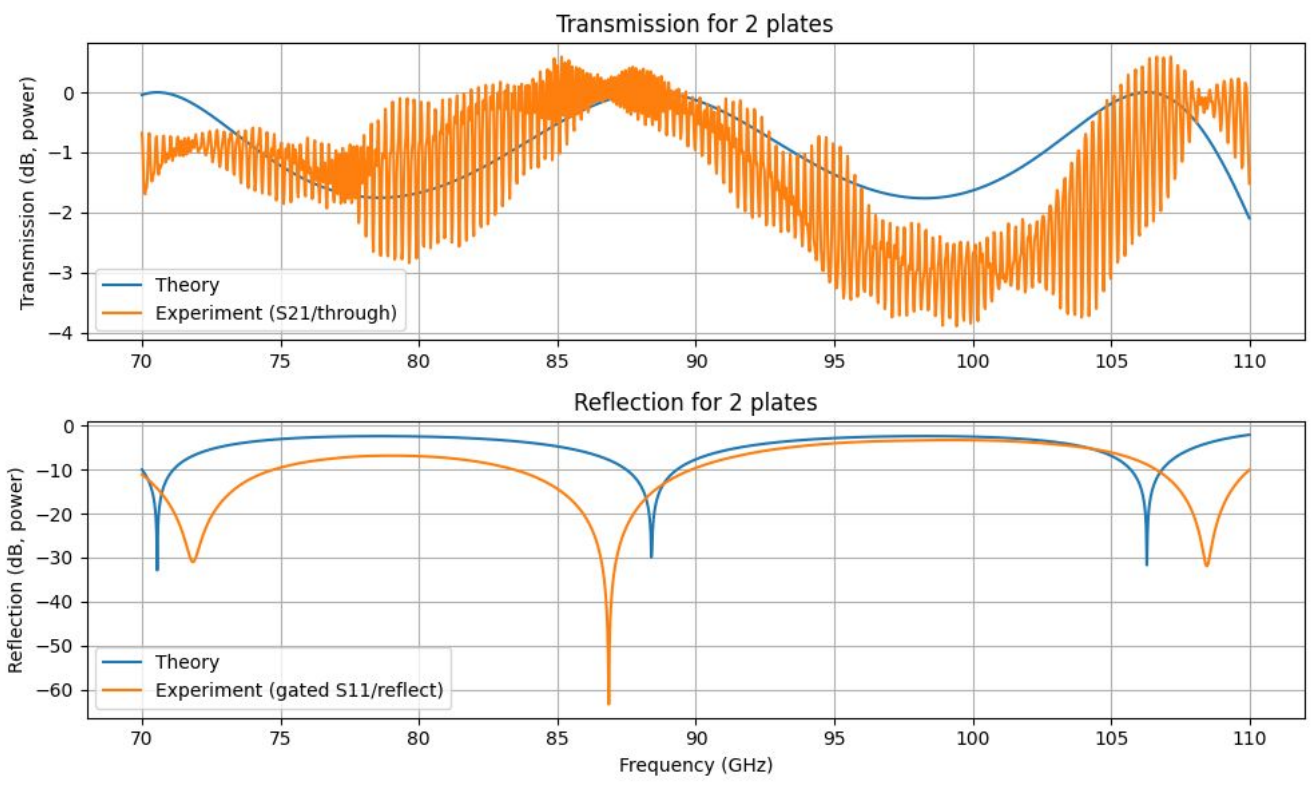

Fig. 15. Transmission (top) and reflection (bottom) data of 2 plate stack composed of high resistivity silicon. Experimental results shown in orange and theoretical prediction shown in blue. Transmission is normalized to through data. Reflection is time gated then normalized.

Comparison to Simulations (5 plates)

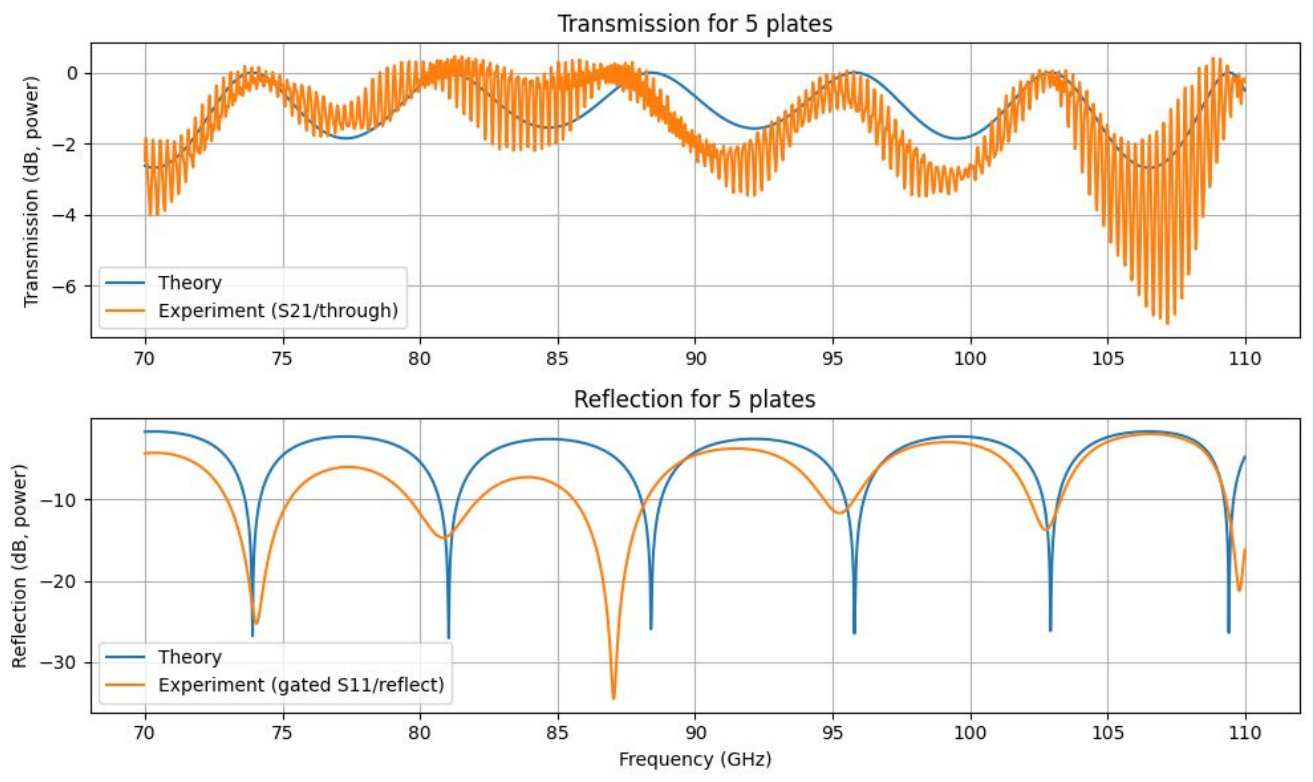

Fig. 15. Transmission (top) and reflection (bottom) data of 5 plate stack composed of high resistivity silicon. Experimental results shown in orange and theoretical prediction shown in blue. Transmission is normalized to through data. Reflection is time gated then normalized.

Fitted Disk Spacing and Angle

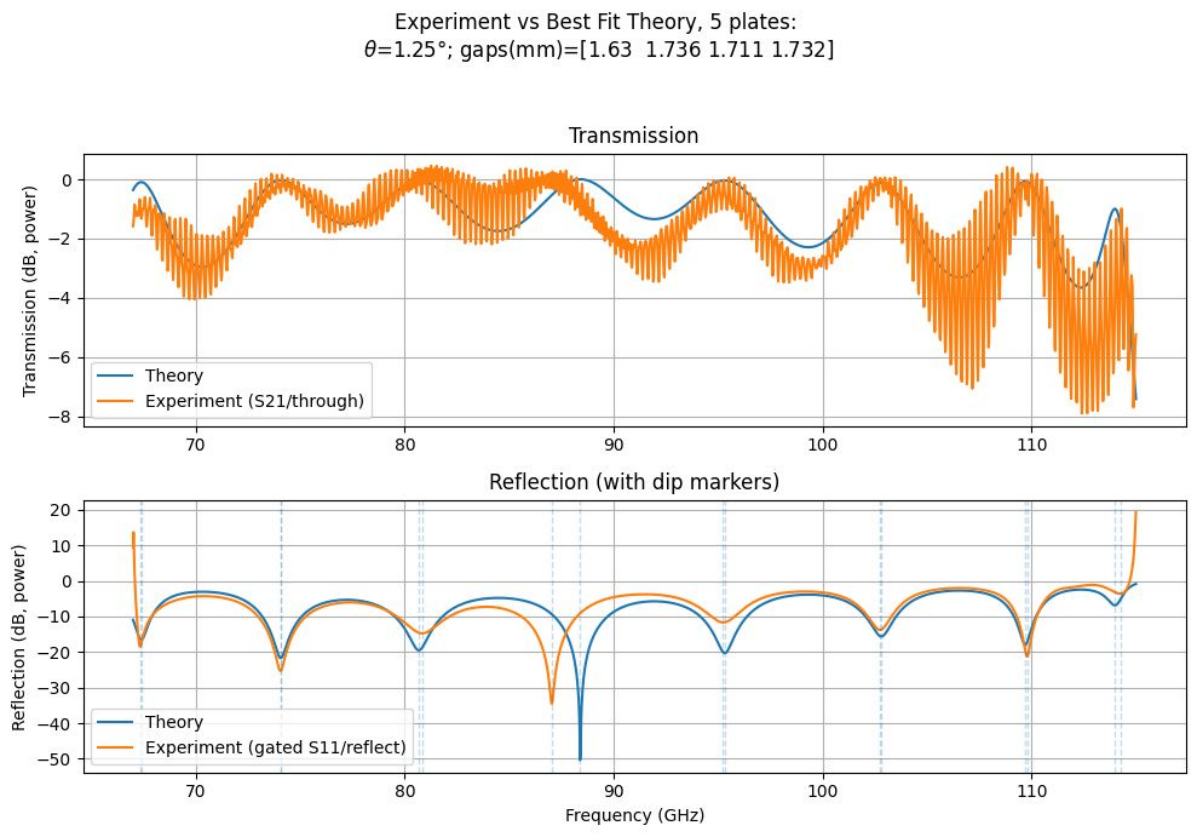

Locations of minima (GHz) (Reflection)

Experiment	Theory Fit
67.336	67.384
74.06	74.06
80.831	80.687
87.05	88.395
95.238	95.31
102.754	102.802
109.789	109.693
114.256	113.991

Fig. 16. Best fit theoretical model vs experimental plots. Fit determined by comparing frequency values of local minima within reflection data.

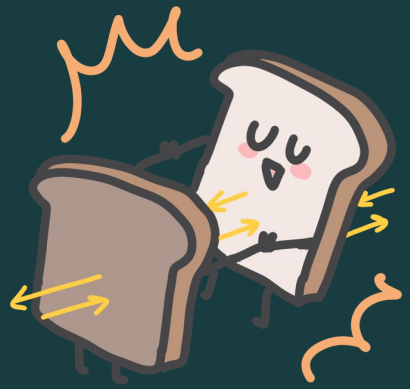

Thank You!

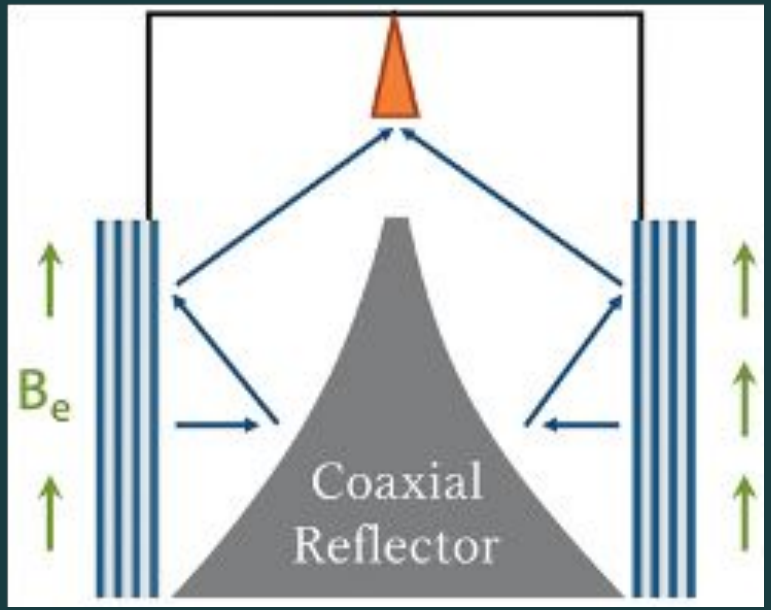

Fig. 17. SlicedBREAD end goal. A cylindrical barrel with walls coated in layers of dielectric material to enhance axion-photon conversion. Photons are then focused onto an antenna by a coaxial reflector.

Future Plans

Short Term:

- Tighter control of plate spacing
- Integration into 4K Cryostat

Long Term:

- Develop geometry of dielectric stacks to integrate into a BREAD-like reflector experiment
- Construct a prototype and perform cryogenic tests in dilution fridge with integrated magnet

Works Cited

“Berkeley Axion Workshop 2025.” *Berkeley Lab Physics Division (Indico)*, https://indico.physics.lbl.gov/event/3134/contributions/9850/.

Born, Max, and Emil Wolf. *Principles of Optics*. 7th (expanded) edition; Sixtieth anniversary edition., Cambridge University Press, 2019.

Caldwell, Allen, et al. “Dielectric Haloscopes: A New Way to Detect Axion Dark Matter.” *arXiv.Org*, 17 Nov. 2016, https://doi.org/10.1103/PhysRevLett.118.091801.

The MADMAX Working Group. “Dielectric Haloscopes: A New Way to Detect Axion Dark Matter.” arXiv:1611.05865, arXiv, 3 Mar. 2017. *arXiv.org*, https://doi.org/10.48550/arXiv.1611.05865.

Backup

Transfer Matrix Formalism

Gives T, R, B for normal incident

usual transfer matrix between in and out EM waves in a 1D system

sum over all axion-induced source terms

$$\begin{pmatrix} R_m \\ L_m \end{pmatrix} = T \begin{pmatrix} R_0 \\ L_0 \end{pmatrix} + E_0 M \begin{pmatrix} 1 \\ 1 \end{pmatrix}$$

$$T = T_0^m \quad \text{and} \quad M = \sum_{s=1}^{m} T_s^m S_{s-1}$$

- calculate the propagation of waves through a multi-layered material.
- each layer changes the amplitude, phase, polarization of the wave
- multiplying a series of matrices describing layers, interfaces in the stacks

Transfer Matrix Formalism

$$G_r = \frac{1}{2n_{r+1}} \begin{pmatrix} n_{r+1} + n_r & n_{r+1} - n_r \\ n_{r+1} - n_r & n_{r+1} + n_r \end{pmatrix}$$

$$P_r = \begin{pmatrix} e^{i\delta_r} & 0 \\ 0 & e^{-i\delta_r} \end{pmatrix}$$

$$S_r = \frac{A_{r+1} - A_r}{2} \begin{pmatrix} 1 & 0 \\ 0 & 1 \end{pmatrix}$$

G: how EM wave changes as it passes from one material to another at the interface (boundary) between materials

P: phase change while it travels through material → affects how the signals combine a

For lossy media: $\tan\delta = \frac{\mathrm{Im}\,\epsilon}{\mathrm{Re}\,\epsilon}$

S: “source term” → EM wave (photons) induced by axions at the interface (how much the axion conversion process affects the signal)

$$A_r = \frac{1}{\epsilon_r} \frac{B_{\mathrm{e},r}}{B_{\mathrm{e,max}}}$$

Boost Factor

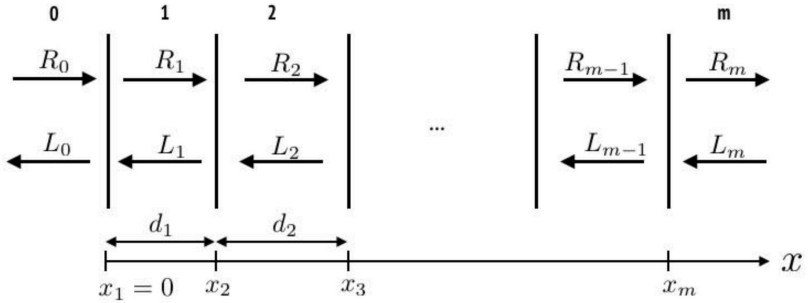

$$L_0 = -E_0 \frac{\mathsf{M}[2,1] + \mathsf{M}[2,2]}{\mathsf{T}[2,2]},$$

$$R_m = E_0 \left(\mathsf{M}[1,1] + \mathsf{M}[1,2] - \frac{\mathsf{M}[2,1] + \mathsf{M}[2,2]}{\mathsf{T}[2,2]} \mathsf{T}[1,2] \right)$$

Boost amplitude: $\mathcal{B}_L = \dfrac{L_0}{E_0}$ and $\mathcal{B}_R = \dfrac{R_m}{E_0}$

Boost factor: $\beta = |\mathcal{B}|$

Max Born, Principle of Optics

Characteristic Matrix

Gives T, R for incident at an angle

$$\boldsymbol{M}(z) = \begin{bmatrix} \cos(k_0 nz\cos\theta) & -\frac{\mathrm{i}}{p}\sin(k_0 nz\cos\theta) \\ -\mathrm{i}p\sin(k_0 nz\cos\theta) & \cos(k_0 nz\cos\theta) \end{bmatrix}$$

$$p = \sqrt{\frac{\varepsilon}{\mu}}\cos\theta \qquad k_0 = \frac{\omega}{c} = \frac{2\pi}{\lambda_0}$$

$$r = \frac{R}{A} = \frac{(m'_{11} + m'_{12}p_l)p_1 - (m'_{21} + m'_{22}p_l)}{(m'_{11} + m'_{12}p_l)p_1 + (m'_{21} + m'_{22}p_l)}$$

$$t = \frac{T}{A} = \frac{2p_1}{(m'_{11} + m'_{12}p_l)p_1 + (m'_{21} + m'_{22}p_l)}$$

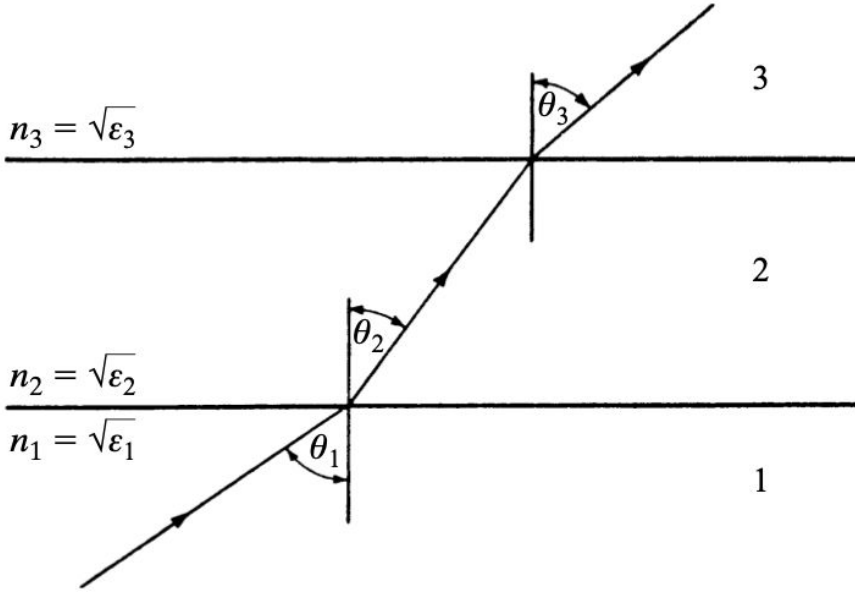

arxiv.org/abs/1612.07057
arxiv.org/abs/2111.12103

Sensitivity for axion

$$\mathcal{L}_a = -\frac{1}{4} g_{a\gamma\gamma} a F_{\mu\nu} \tilde{F}^{\mu\nu}$$

Lagrangian coupling SM photons to axions

$$\left\{ \begin{array}{c} \frac{P_a}{8.8 \cdot 10^{-23}\,\mathrm{W}} \\ \frac{P_{A'}}{2.2 \cdot 10^{-23}\,\mathrm{W}} \end{array} \right\} = \left\{ \begin{array}{c} \left(\frac{g_{a\gamma\gamma}}{10^{-11}\,\mathrm{GeV}^{-1}} \frac{\mathrm{meV}}{m_a} \right)^2 \left(\frac{B_{\mathrm{ext}}}{10\,\mathrm{T}} \right)^2 \\ \frac{\alpha_{\mathrm{pol}}^2}{2/3} \left(\frac{\kappa}{10^{-14}} \right)^2 \end{array} \right\} \times \frac{\rho_{\mathrm{DM}}}{0.45\,\mathrm{GeV/cm}^3} \frac{A_{\mathrm{dish}}}{10\,\mathrm{m}^2}. \quad (8)$$

$$g_{a\gamma\gamma} = \sqrt{\frac{P_a}{8.8 \cdot 10^{-23}\mathrm{W}} \left(\frac{10\mathrm{T}}{B_{ext}} \right)^2 \frac{0.45\mathrm{GeV/cm}^3}{\rho_{DM}} \frac{10\mathrm{m}^2}{A_{dish}}} \cdot \frac{m_a}{\mathrm{meV}} \cdot 10^{-11}\mathrm{GeV}^{-1}$$

$$P_\gamma = \frac{S}{N} k_B T_{sys} \sqrt{\frac{\Delta\nu_a}{\Delta t}} \qquad P_a = \frac{P_\gamma}{\beta^2}$$

$$g_{a\gamma\gamma} \sim \sqrt{\frac{P_\gamma}{\beta^2}}$$

Thermal Contraction

$$\Delta L = \alpha L_0 \Delta T$$

For 0.15 cm clearance (3 in+1.5mm)

```
At 300 K
Disk Diameter: 7.62 cm
Frame outer Diameter: 7.77 cm
Frame inner Diameter: 7.01 cm
Gap: 0.15 cm
```

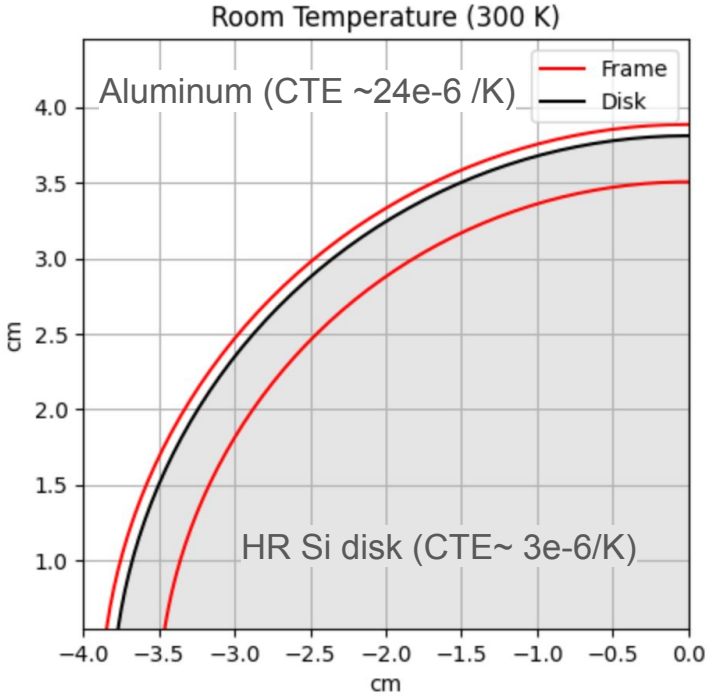


```
At 4 K
Disk Diameter: 7.61 cm
Frame outer Diameter: 7.71 cm
Frame inner Diameter: 6.96 cm
Gap: 0.10 cm
```

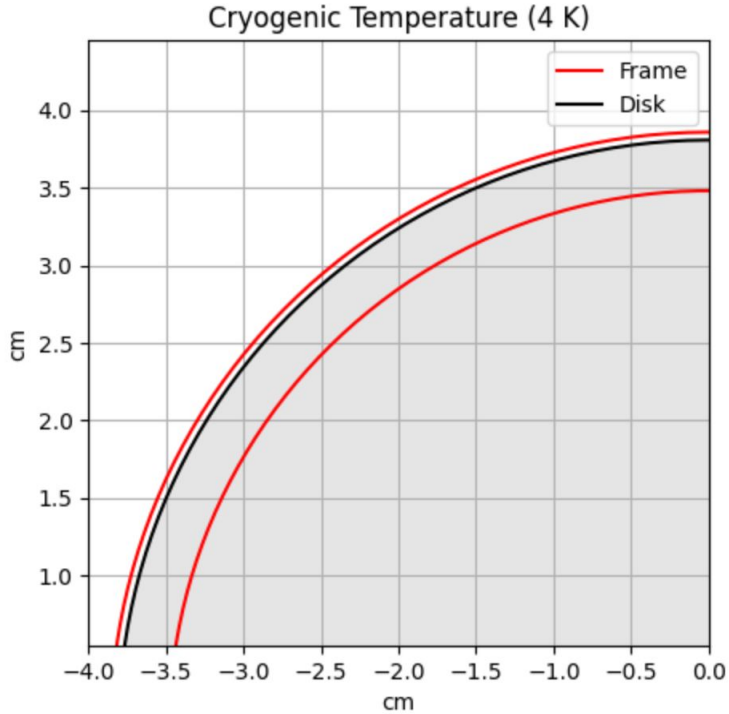

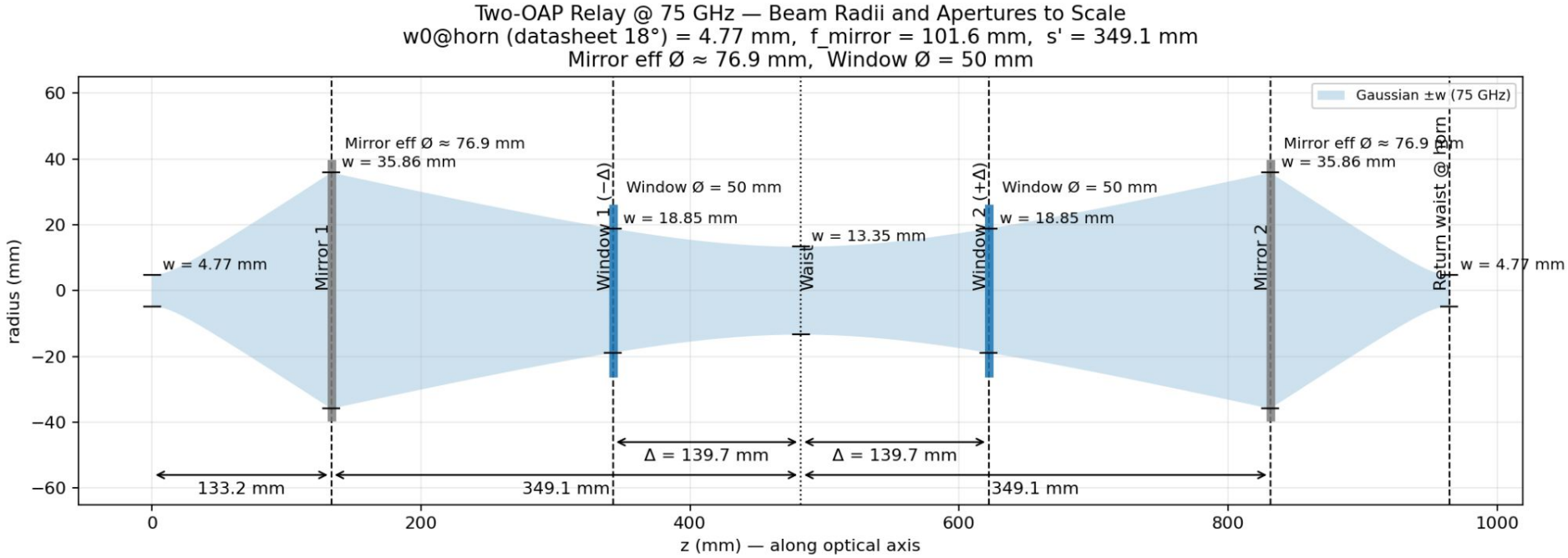
Two-OAP Relay @ 75 GHz — Beam Radii and Apertures to Scale
w0@horn (datasheet 18°) = 4.77 mm, f_mirror = 101.6 mm, s' = 349.1 mm
Mirror eff Ø ≈ 76.9 mm, Window Ø = 50 mm
Gaussian ±w (75 GHz)
Mirror eff Ø ≈ 76.9 mm
w = 35.86 mm
Window Ø = 50 mm
w = 18.85 mm
w = 13.35 mm
Window Ø = 50 mm
w = 18.85 mm
Mirror eff Ø ≈ 76.9 mm
w = 35.86 mm
w = 4.77 mm
Mirror 1
Window 1 (−Δ)
Waist
Window 2 (+Δ)
Mirror 2
Return waist @ horn
w = 4.77 mm
Δ = 139.7 mm
Δ = 139.7 mm
133.2 mm
349.1 mm
349.1 mm
radius (mm)
z (mm) — along optical axis
60
40
20
0
−20
−40
−60
0
200
400
600
800
1000